LOS ALAMOS SCIENTIFIC LABORATORY
of the
University of California

LOS ALAMOS • NEW MEXICO

Quarterly Status Report on the

Advanced Plutonium Fuels Program

October 1 to December 31, 1969

UNITED STATES
ATOMIC ENERGY COMMISSION
CONTRACT W-7405-ENG. 36

This LA-...-MS report presents the status of the LASL Advanced Plutonium Fuels Program. Previous Quarterly Status Reports in this series, all unclassified, are:

LA-3607-MS	LA-3760-MS	LA-4073-MS
LA-3650-MS	LA-3820-MS	LA-4114-MS
LA-3686-MS	LA-3880-MS	LA-4194-MS
LA-3708-MS	LA-3933-MS	LA-4284-MS
LA-3745-MS	LA-3993-MS	LA-4307-MS

This report, like other special-purpose documents in the LA-...-MS series, has not been reviewed or verified for accuracy in the interest of prompt distribution.

Distributed: February 17, 1970

LA-4376-MS
SPECIAL DISTRIBUTION

LOS ALAMOS SCIENTIFIC LABORATORY
of the
University of California
LOS ALAMOS • NEW MEXICO

Quarterly Status Report on the

Advanced Plutonium Fuels Program

October 1 to December 31, 1969

FOREWORD

This is the fourteenth quarterly report on the Advanced Plutonium Fuels Program at the Los Alamos Scientific Laboratory.

Studies on Fast Reactor Metallic Fuels, formerly reported as Project 461 in this series of documents, have been discontinued except for phase-out effort. Any results from the final work will be described under Project 467, a new work category covering all irradiation experiments [chiefly those concerned with (U,Pu)C fuels].

Most of the investigations discussed here are of the continuing type. Results and conclusions described may therefore be changed or augmented as the work continues. Published reference to results cited in this report should not be made without obtaining explicit permission to do so from the person in charge of the work.

CONTENTS

PROJECT 401

EXAMINATION OF FAST REACTOR FUELS

Person in Charge: R. D. Baker
Principal Investigators: J. W. Schulte
J. A. Leary
C. F. Metz

I. INTRODUCTION

This project is directed toward the examination and comparison of the effects of neutron irradiation on LMFBR Program fuel materials. Unirradiated and irradiated materials will be examined as requested by the Fuels and Materials Branch of DRDT. Capabilities are established for providing conventional pre-irradiation and post-irradiation examinations. Additional capabilities include less conventional properties measurements which are needed to provide a sound basis for steady-state operation of fast reactor fuel elements, and for safety analysis under transient conditions.

Analytical chemistry methods that have been modified and mechanized for hot cell manipulators will continue to be applied to the characterization of irradiated fuels. The shielded electron microprobe and emission spectrographic facilities will be used in macro and micro examinations of various fuels and clads. In addition, new capabilities will be developed with emphasis on gamma scanning and analyses to assess spatial distribution of fuel and fission products.

High temperature properties of unirradiated LMFBR fuel materials are now being determined by Contractor in an associated project (ident. no. 07463). Equipment designs and interpretive experience gained in this project are being extended to provide unique capabilities such as differential thermal analysis, melting point determination, high temperature dilatometry, and high temperature heat content and heat of fusion for use on irradiated materials.

II. EQUIPMENT DEVELOPMENT

A. Inert Atmosphere Systems

(C. E. Frantz, J. M. Ledbetter, P. A. Mason, R. F. Velkinburg)

System for Metallography Cells

Argon atmosphere was provided throughout this Quarter to the two metallography boxes and the "blister" where the metallograph is located. Difficulty was encountered initially with the recirculating system when the solenoid values, as supplied by the manufacturer, failed during operation. It was necessary to maintain the inert atmosphere by discontinuing the recirculating system and using Ar from high pressure cylinders on a once-through basis. The approximate average concentrations which were maintained in the containment boxes during this period under these conditions are tabulated below.

TABLE 401-I

O_2 AND MOISTURE IMPURITIES IN INERT ATMOSPHERE OF CONTAINMENT BOXES

	Δp^a of 0.01 in. H_2O^b		Δp^a of 0.03 in. H_2O^c	
Area	O_2, ppm	H_2O, ppm	O_2, ppm	H_2O, ppm
Grinding box	250	20	2000	40[d]
Polishing box	250	20	2500	40[d]
Metallograph Blister	< 5000	150	3000	40[d]

[a] Δp = pressure differential between inside of the containment box and the cell.

[b] The Ar flow rate at this pressure differential was 20 cfh.

[c] The Ar flow rate at this pressure differential was 40 cfh.

[d] This value is probably high as the moisture monitor may have been poisoned by the halogens.

These results demonstrate how sensitive the leak rates are to variations in pressure differential.

The defective solenoid valves were replaced and other improvements in the system were incorporated. Corrosion products found in the system indicate that the Freon TF used in the ultrasonic cleaners may be decomposing in the radiation environment or within the regenerant beds. Efforts will be made to find a suitable solvent as a substitute.

Performance tests on the purifier for the metallography cells revealed that one of the regenerate beds for removing O_2 has been poisoned and will probably have to be replaced. The chemicals for removing H_2O were apparently unaffected.

System for Disassembly Cell

The Ar atmosphere in the containment box used for disassembly of the fuel pins has been maintained generally at ~ 25 ppm O_2 and ~ 10 ppm H_2O using a 50 cfh flow rate and at a pressure differential of nearly 0.0 in. of H_2O (and slightly positive on some occasions).

Performance tests on the recirculating systems are currently in progress for evaluating the efficiency and capacity of the chemical beds.

General Observations

Much valuable experience has been gained during this period in maintaining inert atmospheres within hot cell containment boxes. Based on this experience the following conclusions were arrived at in support of the projected programs:

1. Since the leak rates are very sensitive to pressure differential, it is advisable to develop and install equipment for precisely controlling the differential.
2. A sealed manipulator, such as the CRL Model L, would be beneficial since one of the high suspect leak areas is the plastic booting used on the manipulators for preventing the in-leakage of air and to keep the manipulators from becoming contaminated.
3. The use of an auxiliary Ar system, as mentioned in the preceding Quarterly Report (LA-4307-MS), will be a valuable addition to the present inert gas capability. The design of the high pressure tank system for supplying Ar gas to the containment boxes has been completed. It is anticipated that the installation will be completed by February 15, 1970.

B. In-Cell Equipment

(J. H. Bender, G. R. Brewer, D. B. Court, E. L. Ekberg, F. J. Fitzgibbon, C. F. Frantz, D. D. Jeffries, M. E. Lazarus, J. M. Ledbetter, C. D. Montgomery, T. Romanik, T. J. Romero, A. E. Tafoya, J. R. Trujillo, R. F. Venkinburg, L. A. Waldschmidt)

1. Metallography

The new equipment installed in the inert atmosphere boxes for metallography has functioned quite satisfactorily. Improved results have been obtained in the grinding-polishing, photography, alpha, and beta-gamma autoradiography operations with this equipment. The devices for material transfers between boxes and in and out of boxes have been particularly effective.

A plastic container to fit the 7 in. alpha transfer system has been designed and the first samples received for trial. Preliminary tests appear very promising. These units will save many man-hours in the disposition of Pu-contaminated wastes from the metallography and disassembly cells.

2. DTA

A new remotely-adjustable mirror mount for the optical path from the furnace to the pyrometer was built and installed. Calibrations of the equipment are being completed prior to testing irradiated material. Methods are being explored for an economical way to fabricate tungsten crucibles in the event it is necessary to heat the crucibles in a sealed container.

3. Heat Content

Additional work was done on the drop calorimeter in an effort to determine the reasons for inconsistent calibration values. The apparent heat content of an empty tungsten capsule at 1515°C was determined to be 9.5 kcal/mole with a reference temperature of 25°C.

4. Fission Gas System

During this Quarter, two failures were encountered in the bellows portion of the puncturing device. The cause of the failures was a combination of normal wear on the device, and the thicker wall of the pins being punctured.

A thrust bearing has been incorporated into the puncturing device to obviate any recurrence of this difficulty.

5. Shipping Cask

The 1-1/2 in. diameter holes in the gussets in the base of cask DOT SP 5885 were filled and welded to preclude their use as potential tie-downs or lifting holes.

There are now three types of inserts available for the shipping of irradiated capsules. The diameters and numbers of 40-in. long capsules which can be handled are as follows:

TABLE 401-II

INSERTS FOR SHIPPING CASK

Insert No.	No. of Capsules	Diam. of Capsule, in.
1	19	0.37
2	6	1.13
3	7	0.75

Experience gained on the 5 shipments made thus far indicate a few minor changes which should be incorporated into the design. Approval will be obtained from the Department of Transportation prior to making these modifications.

III. DP WEST FACILITY
(F. J. Fitzgibbon, M. E. Lazarus, C. D. Montgomery, J. R. Trujillo)

This area which houses four hot cells is being altered to provide space and equipment for the non-destructive examination of fast reactor fuel elements. It is anticipated that the equipment to examine fuel elements at a rate of 150 per year will be operational on July 1, 1970.

A set of preliminary drawings was submitted to the AEC (ALO Office) for approval on November 21, 1969. Bids have been requested on a 1-ton, 3-ton, and 25-ton hoist for the facility.

All of the equipment was removed from Room 401 at DP West to give the contractor unrestricted use of the area during modification. The manipulators were removed and stored at the Wing 9 Facility to protect them from the dust which would be produced during any chipping and drilling operations. Progress made on some of the major equipment requirements is listed in the following sections.

A. Unloading and Handling Equipment

The height of the hook for the 25-ton hoist has been increased from 10 ft to 12 ft to accommodate vertical shipping casks.

Precise locations for the additional holes to be added to the cell faces, ceilings, and walls are being determined well in advance of requests for the final drawings.

The Engineering Department is preparing designs on the: corridor bridge crane; cask cart and rails; bridge system for manipulator hoist; and other support equipment.

B. Gamma Scanning

Modifications, to reflect the latest requirements, are being made to both the Ge-Li detector shield and to the shield support.

Design of the scanning mechanism is nearly completed. Procurement of the commercially-available components has already been initiated, with the longest lead time required for the ball screws.

C. Profilometry

The electro-optical unit for this system has arrived. A few problems have been encountered during the unit check out, which should be corrected by the manufacturer before the end of February. It is expected to use essentially the same design for the scanning mechanism as is planned for the gamma scanner.

A Kollmorgen modular periscope, previously purchased for another program, will function as part of the optical relay system.

D. Gas Sampling System

All of the commercial equipment necessary for sampling the cover gas from the capsules has been ordered and received. The sampling system, in which a drill is used to penetrate the cladding, will be employed for sampling the cover gas in the capsules. It is tentatively planned to obtain fission gas samples from all of the pins by using the sampling apparatus in the inert atmosphere disassembly cell at the Wing 9 Facility.

E. Other Operations

The removal of capsule cladding and Na will be done

according to approved safety practices. Tests are currently in progress to develop methods of separating the pin from the capsule in such a way that there is no exposure of a Na-coated pin to the air (such an exposure would have a decided effect on the condition of the pin cladding). Under consideration are heated oil bath techniques, or auxiliary inert gas systems in which the Na is removed by heating and dissolution.

Disposition of active wastes will be carried out using techniques and equipment similar to those employed in the Wing 9 Facility.

Construction has already started on the two movable tables to be used within the cells.

Procurement of equipment for the macro-photography of the capsules and pins is continuing.

IV. METHODS OF ANALYSIS

Measurement of U and Pu
(J. W. Dahlby)

Controlled-potential coulometric titrations of U and Pu, as part of the chemical characterization of irradiated mixed oxide or carbide fuels, was found previously to be satisfactory for determining Pu in the presence of U. Results for U in the presence of Pu showed a small positive bias of 0.3 to 0.4 relative percent if electrical calibration of the equipment was used. In the measurement of Pu, the current was integrated for the coulometric oxidation of Pu(III) to Pu(IV) at a Pt electrode. A Hg working electrode was used in the titration of U in which the current was integrated as U(VI) was coulometrically reduced to U(IV) following a preliminary reduction of more-easily reduced impurities. Various modifications in the titration cell during repeated titrations of U showed that the cause for the positive bias when electrical calibration was used was retention of a small quantity of solution in a minute pocket around the Pt wire that made electrical contact with the Hg electrode through the wall of the titration cup. Replacement of this Pt wire contact with a contact inserted through the cell cover eliminated the positive bias.

The method was tested further by successfully analyzing an irradiated oxide pellet having low beta and gamma activity levels. The relative precision (1 σ) of the method was 0.07 to 0.08 percent for a single determination of either U or Pu in samples of this type. An irradiated mixed-oxide pellet having undergone about 1 percent burnup was dissolved for testing the method on solutions having higher beta-gamma radioactivity levels.

Gross Gamma Scanning
(J. Phillips and J. Deal)

Locating anomalies and areas of interest for further analyses in irradiated fuel elements is an important use of gross gamma scanning provided the results are obtained quickly to avoid delays in destructive sampling of the fuel capsule. To ensure the required speed, a simple gross gamma scanning system was assembled to complement the complex system for detailed gamma scanning. This simple system uses the scanning mechanism, slit, and lithium-drifted germanium detector of the detailed gamma scanner for accurate resolution of scan position and reliable measurements. An amplifier, single channel analyzer set to accept all gamma energies above a preset background, a scaler timer, and a printer complete the system. Testing of the gross gamma scanner is in progress. Present schedules indicate that use of the gross gamma scanner will not interfere significantly with planned operations of the system for detailed gamma scanning although some components are common to each scanner.

V. REQUESTS FROM DRDT

A. Examination of Irradiated Material
(K. A. Johnson, J. R. Phillips, J. W. Schulte, J. F. Torbert (GMX-1), E.D. Loughran (GMX-2), G. R. Waterbury)

Battelle Northwest Laboratory

From each of the pins BNW-1-9, -11, and PNL-1-15, 17, 19, two tube burst test specimens were prepared and packaged in an inert atmosphere in Swagelok fittings provided by BNWL personnel. These specimens together with two fuel samples from PNL-1-19 were shipped to BNWL on October 30.

Table 401-III lists the metallographic work completed this Quarter on one transverse section (fuel and clad) from each of the pins listed. Samples were prepared and examined in an inert (Ar) atmosphere.

TABLE 401-III

METALLOGRAPHIC EXAMINATION OF BNWL MATERIALS

Pin	Macrophotos	α Auto-radiography	β-γ Auto-radiography	Optical Metallography	Replication
PNL-1-15	X	X	X	X	
PNL-1-16	X	X	X	X	X
PNL-1-17	X	X	X	X	
PNL-1-18	X	X	X	X	X
PNL-1-19	X	X	X	X	
BNW-1-9	X	X	X	X	
BNW-1-11	X	X	X	X	
PNL-X-1	X	X	X	X	X
PNL-X-3	X	X	X	X	X
PNL-X-4	X	X	X	X	X
PNL-X-6	X	X	X	X	X
PNL-X-7	X	X	X	X	X

Electron microprobe examinations were completed on a cross section from each of two fuel pins, PNL-1-17 and BNW-1-11.

Data reports were forwarded to the Sponsor as different phases of the work were completed.

United Nuclear Corporation

Work was started again on 3 UNC pins which had been taken through the profilometry when operations were curtailed in favor of higher priority specimens. The following tests were performed on UNC-87, -89, and -90:

1. Fission gas samples were taken and analyzed from UNC-87; some difficulty was encountered in getting good samples from each of the 4 segments of UNC-89 and -90.
2. Dissection to remove Nb discs, Fe monitor wires, and fuel samples.
3. Density tests by immersion were run on 3 pellet fragments from UNC-89.

On October 29, 3 capsules, UNC-81, -82, and -83 were received from the EBR-II. The following operations were performed on these capsules:

1. Visual inspection and photography.
2. Measurements for contamination and radiation.
3. Temperature measurements.
4. Radiography.
5. Micrometer measurements.
6. Gamma scanning.
7. Sampling of cover gas (UNC-81 only).

In Table 401-IV is listed the metallographic work completed this Quarter. These samples were also

TABLE 401-IV

METALLOGRAPHIC EXAMINATION OF UNC MATERIAL

Pin Section	Type	Macrophotos	α Auto-radiography	β-γ Auto-radiography	Optical Metallography
UNC-87-1	Nb disk	X	X	X	X
UNC-87-2	" "	X	X	X	X
UNC-87-A	Fuel + Clad	X	X	X	X
UNC-87-D	" "	X	X	X	X
UNC-87-E	" "	X	X	X	X
UNC-87-I	" "	X	X	X	X
UNC-87-CM-1	Plenum Clad	X	X	X	X
UNC-89-1	Nb disk	X	X	X	X
UNC-89-2	" "	X	X	X	X
UNC-89-3	" "	X	X	X	X
UNC-89-4	" "	X	X	X	X
UNC-89-C	Fuel + Clad	X	X	X	X
UNC-89-H	" "	X	X	X	X
UNC-89-M	" "	X	X	X	X
UNC-89-R	" "	X	X	X	X
UNC-90-1	Nb disks	X	X	X	X
UNC-90-2	" "	X	X	X	X
UNC-90-3	" "	X	X	X	X
UNC-90-4	" "	X	X	X	X
UNC-90-C	Fuel + Clad	X	X	X	X
UNC-90-H	" "	X	X	X	X
UNC-90-M	" "	X	X	X	X
UNC-90-R	" "	X	X	X	X

processed in an inert atmosphere (Ar).

Eleven iron, flux-monitor wires from capsules UNC-87, -89, and -90 were dissolved in-cell, and aliquots were taken for radiochemical determinations of absolute counting rates.

Electron microprobe examination was started on a cross section of pin UNC-87. A silver stripe was painted remotely from the edge of the mount to the edge of the specimen to provide the necessary conductive path. Heretofore, a carbon coating had been evaporated on the surface of the mount and specimen to provide conductivity. Either method has been shown to produce satisfactory results.

Cask DOT SP-5885 was provided to Douglas-United Nuclear for shipping some irradiated (U, Pu)C experimental assemblies from the Hanford area to ANL-Illinois. These were originally destined to be examined at LASL, but since the fuel was Na-bonded, DRDT directed that they be shipped to ANL.

Data reports were forwarded to the sponsor as usual when phases of the work were completed.

Westinghouse (WARD)

Processing of gamma scanning data for three

capsules (W-1-G, W-2-G, and W-3-G was continued.

An insert for the LASL shipping cask was designed and fabricated for transferring these three WARD capsules to ANL-Illinois. It was also decided by DRDT to examine these Na-bonded fuel pins at ANL.

Atomics International

An additional 4 replicas from the (W-U)C specimens were sent to AI for evaluation. This completes the six specimens which DRDT authorized LASL to prepare. The gamma scan data analysis on the monitoring wires was completed and the report forwarded to AI. Assuming the 3 samples sent to Idaho Nuclear for burnup analysis are satisfactory, LASL has completed its commitments in regard to this experiment.

Nuclear Materials and Equipment Company

Three NUMEC capsules were received from the EBR-II on October 29. Two of these capsules were to be shipped to NUMEC at a later date, and one (NUMEC B-11) was to be examined at LASL. After receipt of two capsules at Quehanna, NUMEC was to forward three pins (partially examined) to LASL. One of these three pins was for examination at BNWL at some future date, and the remaining two would be examined at LASL as scheduled by DRDT.

The following non-destructive tests were completed on the NUMEC B-11 capsule:

1. Visual inspection.
2. Contamination, radiation and temperature measurements.
3. Radiography.
4. Micrometer measurements.
5. Center point of balance.
6. Photography.

Additional examinations will be carried out after discussions are held with NUMEC personnel and approval is received from DRDT for the proposed work.

LASL (K-Division)

Experiment OWREX 13 was received from the OWR. A radiation reading of 15 rhm on this unit indicated that the examination would have to be carried out in a hot cell when it could be scheduled into the program.

VI. EXAMINATION OF UNIRRADIATED FUELS

(J. A. Leary, M. W. Shupe, E. A. Hakkila, R. T. Phelps, G. R. Waterbury, K. A. Johnson)

Westinghouse Advanced Reactor Division

Metallography and electron microprobe analyses were completed on mixed carbide pellets, S-6, X-6, and on one pellet each from batches 549, 539, and 536.

VII. PAPERS PRESENTED

"Containment Boxes for Plutonium Fuels Examination," C. D. Montgomery, 17th Conference on Remote Systems Technology (American Nuclear Society) December 1-4, 1969, San Francisco, California.

PROJECT 462

SODIUM TECHNOLOGY

Person in Charge: D. B. Hall
Principal Investigator: J. C. Biery

I. INTRODUCTION

For the successful operation of high temperature sodium systems contemplated for use in fast, central station reactor concepts, impurities in the sodium must be monitored and controlled. Nonradioactive impurities such as oxygen must be maintained at low concentration levels to limit corrosion processes. To control the levels of these impurities, a knowledge of their behavior and interactions in sodium must be developed.

The sodium technology program at LASL has projects directed toward acquiring information about and designing equipment for the control and monitoring of impurities with precipitation processes. Also, equipment is being designed to sample sodium cover gas at operating temperatures with a quadrupole mass spectrometer. The current LASL projects are summarized below.

A. Study and Design of Precipitation Devices
   1. Study of Plugging Meter Kinetics
B. Sampling and Analysis
   1. Development of a High Temperature Quadrupole Mass Spectrometer for Cover Gas Analysis
   2. Total Carbon Analysis Development

The following projects are being phased out because of funding reductions and will be reported here as the final data are generated and analyzed.

C. Phaseout Programs
   1. Study of Carbon Transport in Thermal Convection Loops
   2. Study of Gas Diffusion Through Metals
   3. Study of Soluble Getters in Sodium
   4. Study of Sodium Leaks
   5. Development of Remotely Operated Distillation Sampler for EBR-II
   6. Analysis of Dynamic Cold Trap Performance

II. STUDY AND DESIGN OF PRECIPITATION DEVICES

A. Study of Plugging Indicator Kinetics
(J. C. Biery, D. N. Rodgers, W. W. Schertz, J. L. Bacastow)

1. General

Plugging meters have been used on sodium systems for many years. They are relatively simple to design, install, and operate; however, the meaning of the data obtained from these instruments has not always been clear, and, as a result, the value of the instrument has sometimes been questioned in the past. Previously reported LASL work[1] indicates, however, that the plugging meter is a valuable instrument and that it can be used with confidence. The three areas of investigation indicated below are continuing in order to better understand and use the meter.

(a) Characterization of the plugging indicator's dynamic behavior with type of impurity.

(b) Studies of orifice configurations and materials to improve nucleation and dynamic characteristics at low concentrations (~1 ppm or less range).

(c) Development of a prototype plugging indicator system incorporating the research results of (a) and (b).

2. Current Results

The plugging meter research program at LASL is being conducted in two loops; Plugging Indicator Loop No. 1 (PIL-1), formerly named Analytical Loop No. 2, and Plugging Indicator Loop No. 2 (PIL-2), formerly named Cold Trap Loop. The characteristics of the two loops are summarized in the previous quarterly report.[2]

a. Research in Plugging Indicator Loop No. 1 - (PIL-1)

(1) PIL-1 Operation

After nearly one month of isothermal operation at 350°C with a saturation temperature of 190°C, as indicated by the "oscillating" plugging meter, cold trapping was begun on October 22, 1969. By November 7, 1969, the system was being cold trapped at 120°C. Cold trapping at 120°C has continued to the present time to remove impurities in preparation for the first single impurity plugging indicator runs using oxygen.

When cold trapping was begun, the helium cover gas was flushed several times to bring the impurity levels below ~3 ppm (H_2, O_2 + Ar, N_2, CH_4). Presently, about 16 ppm H_2 and 1 to 2 ppm N_2 are the only observed impurities.

(2) History of Impurities in Cover Gas of PIL-1

The history of impurities in the cover gas are summarized in Table 462-I. These data, when combined with oxygen distillation results reported previously,[2] give considerable information about the behavior of the impurities in the sodium.

Oxygen

No oxygen has been detected in the cover gas; however, the vacuum distillation results showed the apparent oxygen level in the sodium to start at 10 ppm by weight on July 3, 1969, and decrease to 4.8 ppm by weight by July 30, 1969. The 4.8 ppm by weight correlated well with the 190-195°C saturation temperature indicated by the "oscillating" plugging indicator. (The Rutkauskas[3] oxygen solubility curve gives an oxygen saturation concentration of 4.6 to 5.9 ppm by weight for 190-195°C saturation temperature.) The initial high "oxygen" concentration implied that the sodium contained an impurity that did not decompose in the vacuum distillation process and that this impurity disappeared as of July 30, 1969. When cold trapping in the 110-120°C range was initiated, the oxygen concentration by vacuum distillation dropped below 1.0 ppm by weight.

Hydrogen

The partial pressure of hydrogen remained constant from June 25, 1969, through October 21, 1969, at which time cold trapping was initiated. The average hydrogen concentration over this period was 42 ppm by volume which corresponds well with the expected 36 to 50 ppm by volume for saturated NaH solutions at 190-195°C.[4] Thus, the vacuum distillation results and the hydrogen partial pressure indicate that at least two impurities, Na_2O and NaH, were saturated at the saturation temperature shown by the "oscillating" plugging meter.

Also, since the H_2 partial pressure remained constant up to October 21, 1969, the excess "oxygen" concentration indicated by vacuum distillation could not be due to NaH. The "excess" oxygen decreased about August 1, 1969, with the NaH concentration remaining constant.

When cold trapping was initiated, the H_2 concentration dropped to a level that was undetectable. At 150°C the partial pressure should be approximately 2 ppm by volume and at 120°C, 0.25 ppm by volume.[4] Thus, most of the NaH appeared to be removed in the cold trap. However, after running for a month some H_2 (~10 ppm by volume) appeared in the cover gas. This increase may imply that NaH may be deposited above the sodium meniscus in the bulk hold tank and is unavailable for removal in the cold trap.

Methane

The methane concentration remained in the 15 to 37 ppm by volume range until August 4, 1969, at which time the second cover gas flush was effective in reducing the concentration to 3 ppm by volume. This drop corresponds closely to the decrease in excess "oxygen" concentration by vacuum distillation. Thus, the compound that did not decompose in vacuum distillation may well be carbon bearing. The ratio of CH_4 in the cover gas to excess "oxygen" in the sodium was approximately 7:1 in ppm by volume CH_4/ppm by weight "oxygen." If the carbon compound were Na_2C_2, the ratio would be 4.5:1 ppm by volume CH_4/ppm by weight carbon in sodium as Na_2C_2.

When cold trapping started, the methane concentration dropped to zero and was undetectable for the next two months. Two possibilities might explain the decrease: (1) The carbon-bearing compound is precipitable; (2) Since hydrogen is necessary to produce CH_4 from a compound such as Na_2C_2, the production of CH_4 stopped when the concentration of NaH decreased to near zero with the initiation of the cold trapping.

Table 462-I

Summary of Cover Gas Impurities Concentrations in PIL-1

Date (1969)	Average Impurity Concentration ppm by volume H_2	CH_4	N_2	No. of Samples	Bulk Sodium Temp. - °C	Saturation Temp. - °C	Operation
6/19-6/24	72	25	4	4	165	190-195	
6/25-7/14	42	36	11*	7	225	190-195	
7/14-7/15							Flushed cover gas
7/16	40	14	0	1	225	190-195	
7/17-7/28	40	23	8*	4	250	190-195	
7/29-8/4	38	37	20	5	300	190-195	
8/4							Flushed cover gas
8/4-8/11	32	2.4	1.4*	6	300	190-195	
8/12-9/8	49	2.8	1.7	13	350	190-195	
9/11							Flushed cover gas
9/12-10/20	51	6.0	11.0*	10	350	190-195	
10/20							Flushed cover gas
10/21-11/3	0	0	1.1*	3	350	150-160	Cold trapping - 150°C
11/3-12/29	9	0	2.8*	17	350	~120	Cold trapping - 106-125°C Flushed gas space five times in the time period.

*Concentration steadily increased after each flushing of the cover gas.

Nitrogen

The nitrogen concentration did not correlate with sodium temperature or cold trapping temperature. The concentration dropped to near zero with each cover gas flushing and slowly increased with time. This behavior implied that a very small leak existed or some N_2 diffusion through the stainless steel was occurring.

Conclusions

Two impurities, Na_2O and NaH were saturated in the sodium at 190-195°C. Both were removed by cold trapping. Also, the sodium contained a carbon-bearing compound that may have been responsible for producing "high-oxygen" vacuum distillation results. Methane, which indicated the existence of the carbon compound, disappeared when cold trapping was initiated.

(3) Plugging Meter Operation During Cold Trapping

As cold trapping proceeded, the nature of the plugging indicator oscillations changed dramatically. At 190°C saturation temperature, the flow oscillations were well developed and varied from 0.07 to 0.14 gpm. When the cold trap was run at 150°C, the flow oscillation amplitude decreased considerably and varied between 0.105 and 0.113 gpm. At a cold trap temperature of 115°C, further damping occurred with the flow varying between 0.105 and 0.110 gpm.

Some qualitative observations can be made from the data at the 190°C saturation temperature and the two cold trap temperatures of 150 and 120°C: (1) The kinetic behavior at the 190°C saturation temperature indicated, at least qualitatively, that only one impurity was precipitating. (2) With a cold trap temperature of 150°C, the flow trace indicated that possibly two impurities were precipitating on the orifice - one with a saturation temperature in the 160-170°C range and a second one in the 110-125°C range. The minima in flow consistently indicated the second impurity while the maxima indicated the first. A change in slope during precipitation also indicated the possibility of a lower saturation temperature impurity. Also, the rates of precipitation were much slower than the rates of dissolution. Mass transfer coefficient

analysis will indicate whether the different rates are a result of a changing mechanism or alternatively of the lower concentration driving force available below the lower saturation temperature.

(3) At the 115°C cold trap temperature, again only one impurity was found; its saturation temperature was in the 115-125°C range. Again, the dissolution rate was faster than the precipitation rate.

(4) Modifications to PIL-1

Two stacked Powerstat units have been reconditioned and installed to replace the single units which supplied power for the automatically and manually controlled bulk tank heaters. The new stacked units nearly double the available heater power and allow operation of the loop at 400°C which was not previously possible.

The resistivity meter side loop was removed and replaced with a removable orifice plugging indicator loop. The new plugging indicator will be used to collect precipitated material for analysis and to test different orifice designs. The new side loop will not be operational until trace heater installation and insulation is completed.

The same solids addition device that was used successfully on Analytical Loop No. 1 will be used on PIL-1. An additional component is required, however, on the inside of the PIL-1 bulk tank to retain the solids addition basket assembly for retrieval. This component was fabricated and installed and is now ready for operation.

(5) Preparation for Na_2O Addition to Loop

After cleanup of the loop, oxygen is to be added as Na_2O to start a series of plugging indicator runs with a known source of oxygen. The Na_2O will be added through the solids addition mechanism which has now been assembled and installed in the main tank of the loop.

A source of solid Na_2O was obtained and analyzed to determine its composition. Seven samples of the material were dissolved in water and titrated. The titrated solution was then analyzed spectrophotometrically for Na^+. Both analyses indicated that the material is a heterogeneous mixture of metallic sodium and Na_2O (10% sodium and 90% Na_2O). Sodium carbonate was not detected (<0.5%), and the results indicate the NaOH concentration to be low. The material is of sufficient quality to be used as a hydrogen-free source of oxygen for future plugging meter experiments in PIL-1.

b. Research with Plugging Indicator Loop No. 2 - (PIL-2)

(1) Plugging Indicator Runs

Several interesting plugging indicator runs were performed on the loop during the reporting period. These are summarized below.

Run 10369

The plugging meter orifice temperature was increased sufficiently above the indicated 190°C saturation temperature to allow the plug that was present to partially dissolve. The temperature was then dropped to 181°C. The flow maintained a steady value for 10 min, and then decreased at a constant rate. The period of constant flow is most probably explained by a two-impurity system in which one of the species (impurity 1) is precipitating and the other (impurity 2) is dissolving at equal rates. When the dissolving impurity (No. 2) is sufficiently covered with the precipitating impurity (No. 1), the dissolution stops and flow decreases. After an extended period (~1 h) of steady precipitation, the temperature was dropped to 160°C. An increase in the rate of precipitation was noted. This change could have been due to an increase in driving force for precipitation of impurity No. 1 or to the initiation of precipitation of impurity No. 2.

To help clarify the possible two-impurity behavior, data from this run were analyzed with the aid of the computer program, PLUGIN, and the results are summarized in Table 462-II. The primary impurity was assumed to be oxygen with a saturation temperature of 190°C. It should be noted that the rate constant (k) is lower than the values usually found for oxygen and that the rate constant increased significantly when the orifice temperature was dropped to 160°C. This behavior is not consistent with the concept of a single impurity since k should be relatively independent of driving force. Therefore, at least two impurities are indicated, impurity No. 1 having a saturation temperature above 181°C, and impurity No. 2 having a saturation temperature between 160 and 181°C. These data were not reanalyzed using the lower estimated saturation temperature.

Table 462-II

Mass Transfer Coefficients for Run 10369

Orifice Temperature, °C	Rate Constant (k) (g O/(ppm-h-cm^2)
181	7.7×10^{-4}
181	5.0×10^{-4}
181	7.2×10^{-4}
160	20.7×10^{-4}
160	20.0×10^{-4}
160	13.3×10^{-4}
160	21.6×10^{-4}

Run 101369

The impurities in the cold trap were dissolved off, and, as a result, the saturation temperature indicated by the oscillating plugging meter increased to ~206°C. Maintaining the orifice at 207°C resulted in a very slow dissolution of the plug on the orifice. (Presumably, impurity No. 1 was dissolving.) Then, the temperature was dropped to 160°C to deposit the lower saturation temperature impurity (No. 2) on the orifice. After an extended period of precipitation, the temperature was raised back to 207°C. The flow increased as impurity No. 2 dissolved until the original flow was established at which point the dissolution stopped. This behavior indicated that very little of impurity No. 1 was deposited in this time span while the second impurity was precipitating and dissolving.

To determine the saturation temperature of impurity No. 2, a constant temperature run similar to the above was made at an orifice temperature of 175°C. The curves were analyzed with PLUGIN, and the saturation temperature in the program was varied until the same rate constant was obtained for the two constant temperature precipitation runs (160 and 175°C orifice temperatures). This technique represents a useful procedure for analyzing plugging indicator responses with multiple impurities. The results are presented in Table 462-III and indicate that the saturation temperature for impurity No. 2 was about 186°C. The impurity assumed in the calculation was oxygen. (NOTE: The use of another solubility curve such as that of NaH would have changed the numerical results because of the differing slopes of the curves; however, qualitatively the result would have been similar.)

Table 462-III

Mass Transfer Coefficient Variation with Changes in the Estimated Saturation Temperature of the Lower Temperature Impurity - Run 101369

Assumed Saturation Temperature	k(160°C precipitation)	k(175°C precipitation)
180	4.5×10^{-3}	7.75×10^{-3}
185	3.25×10^{-3}	3.58×10^{-3}
186	3.05×10^{-3}	3.13×10^{-3}
190	2.45×10^{-3}	2.15×10^{-3}

Run 111369

The impurities in the loop were removed by cold trapping to a saturation temperature of 105°C. The plugging indicator worked satisfactorily during the cleanup and indicated a final saturation temperature in the 105-110°C range.

The flow through the cold trap was valved off and the system flow was established through the overflow line in the expansion tank to dissolve any impurities present on the walls above the normal gas/liquid interface level. After two days of operation (with the sodium temperature at 150°C) very little increase in the saturation temperature was noted.

Run 111869

The plug was lost from the orifice during a maintenance shutdown and several days were required to re-establish the impurity on the orifice due to the extremely low saturation temperature. On November 18, 1969, a plug was established and a saturation temperature of 120°C was indicated. The sodium had been pumped through the expansion tank overflow line for two days at over 300°C sodium temperature. Thus, at 300°C the rate of dissolution of impurities from the walls of the gas space was approximately equal to the deposition rate in the cold trap.

The heat input was then increased to raise the system temperature up to 450°C. The plugging indicator operated in the automatic mode and indicated the varying saturation temperatures of the system. The concentration of the impurities increased overnight to a level above the range of the plugging indicator at the power settings used. By increasing the heat input to the plugging indicator, a saturation temperature of ~380°C was obtained. Table

462-IV shows the buildup of impurity with time for the system operated in an expansion tank overflow configuration at 450°C. At this temperature the cold trap was continuously in operation, and it could not remove the impurities as fast as they were being dissolved by the 450°C sodium from the walls of the expansion tank.

This increase in concentration with liquid overflow from the expansion tank is definite proof of the existence of impurities on the walls of the tank in the gas phase. The presence of such deposits can lead to ambiguous results when oxygen is added to or removed from the system and an oxygen balance is attempted.

Table 462-IV

Saturation Temperature Versus Time for PIL-2 with System Temperature of 450°C and Sodium Overflowing from the Expansion Tank

Date	Time	Saturation Temperature - °C
11/18/69	1600	126
	1700	117
	1800	122
	1900	126
	2000	130
	2100	126
	2300	143
	2400	149
11/19/69	1000	363
	1900	355
11/20/69	0200	376-380

Run 121569

The system was cleaned up with the water-cooled cold trap, but the existing plug on the plugging indicator orifice was lost due to a momentary stopping of the main system flow. By careful adjustment of the plugging indicator cooling and heating rates, the bare orifice was run at ~100°C for three days and a plug was finally formed. A saturation temperature of 107°C was indicated. This saturation temperature was maintained for two weeks with no change. This was the first time at LASL that it had been possible to form an impurity plug on a bare orifice when the saturation temperature of the impurity was below 120°C.

(2) Summary of Results of Plugging Indicator Runs in PIL-2

During the report period, the plugging indicator has again been demonstrated to be an effective instrument for following transients of impurity concentrations in sodium systems. Under certain conditions, it can be used to detect multiple impurities, and stable oscillatory behavior has been demonstrated for saturation temperatures from 380 to 105°C. Also, a new plug was formed on a bare orifice with a saturation temperature of 107°C.

It has been shown that impurities can deposit on the walls of the gas phase region of a sodium system. These impurities can complicate the interpretation of cold trap rate data and oxygen addition studies. These impurities can be washed from the walls with flowing sodium and subsequently be removed from the system by cold trapping.

III. SAMPLING AND ANALYSIS

A. Development of a High Temperature Quadrupole Mass Spectrometer for Cover Gas Analysis (J. P. Brainard, C. R. Winkelman)

1. General

The purpose of this research is to develop a method for continuous on-line analysis of high temperature (up to 650°C) cover gas in an LMFBR. The analyzer must be capable of detecting impurities such as nitrogen, oxygen, hydrogen, carbon dioxide, methane, and fission products in the cover gas with a sensitivity varying from the part-per-million range to the percent range. A response time of about 1 min is necessary if the analytical data are to serve as an error signal for activating devices for continuous control of cover gas composition.

A quadrupole mass spectrometer was obtained in order to meet the above requirements. It is believed that reasonably representative sampling can be accomplished by transporting the sample gas in sodium loop containment materials and at sodium loop temperatures until it has passed through the spectrometer for analysis.

2. Current Results

The analyzer design is complete and the fabrication of parts is scheduled for completion in January, 1970. A mechanical beam chopper has been ordered, and the manufacturer has verified that the beam chopper can meet the high temperature and high vacuum specifications. A layout drawing has been completed to show the volume available for locating

and mounting the beam chopper. A lock-in amplifier for use with the signal generated by the chopped beam has been ordered. A paper on the gas analyzer is being written; it will include information on the response time and sensitivity which can be expected with this analyzer.

The machining of spherical dies needed for the gas analyzer fabrication has produced a new production technique for generating surfaces with cylindrical symmetry. A draft of a paper on this work has been completed.

B. Analysis Development
(K. S. Bergstresser)

1. General

The low temperature combustion technique for analysis of total carbon of sodium is being refined. By using a high sensitivity gas chromatograph for quantitative measurement of the carbon dioxide produced, it is hoped that carbon concentrations in the 1- to 10-ppm range can be determined.

2. Current Results

Recent investigation was concerned primarily with separation of trace amounts of carbon dioxide from the products of combustion of sodium in oxygen at relatively low temperatures.[5] A bubbler tube was used to remove carbon dioxide from an acidified solution of the sodium oxide by sweeping with a stream of helium in the form of fine bubbles. This gas was then partially dried over anhydrous $Mg(C\ell O_4)_2$ and transferred to the gas chromatograph for measurement. A valving system and auxiliary chromatographic column were installed to complete the removal of moisture from the helium carrier gas. The entire system was put into operation, and various methods for transfer of the oxidized sodium samples to the bubbler tube were tested. Operating experience indicated that the system was too complex for routine analyses. For this reason, investigation was started of an alternate method in which acid was added directly to the nickel chamber used for combustion of the sodium, and aliquots of only the gas phase were withdrawn for measurements of carbon dioxide content.

IV. PROJECTS BEING PHASED OUT

Status of programs which are being phased out because of funding cuts are discussed below. Results obtained during the orderly conclusion of these tasks will appear here until the work has terminated.

A. Study of Carbon Transport in Thermal Convection Loops
(J. C. Biery, J. R. Phillips)

1. General

Studies have indicated that the use of carbon beds may be useful in the gettering of ^{137}Cs in sodium systems. Carbon, however, is slightly soluble in sodium and can carburize austenitic stainless steels and refractory metals. Therefore, the purpose of this study is to determine the conditions, if any, under which carbon mass transfer rates are sufficiently low to allow the use of carbon beds in a sodium system.

The carbon transfer rates from carbon rods are being studied in thermal convection loops. The Type 304 stainless steel loop itself is serving as the carbon sink.

2. Current Results

As of December 31, 1969, 7,324 h of run time have been accumulated on the thermal harp. A summary of the times at various temperatures is presented in Table 462-V.

Table 462-V

Temperature - Time Summary - Thermal Convection Harp

No. of Hours	Temperature - °C	
	Hot Leg	Cold Leg
336	485	455
1608	520	480
5020	510	450
360	330	130

This experiment will be continued until 8,000 h of run time are accumulated. The loop will be destructively examined to determine the extent of the carbon mass transfer.

B. Study of Gas Diffusion Through Metals
(J. P. Brainard)

1. General

Very little quantitative information is available on the diffusion of gases in reactor system containment materials, although the phenomenon has been observed in several high temperature, liquid-metal-cooled systems. Diffusion of nitrogen through stainless steel in such systems may be misinterpreted as evidence of an air leak in the plumbing. If quantitative information on diffusion were available, the expected rate of nitrogen influx could be estimated, and the existence of small hard-to-find

leaks might be substantiated or dismissed by comparing the expected and observed rates of nitrogen accumulation in the system.

2. Current Results

Nitrogen permeation through stainless steel experiments have been run with the temperatures at 278, 433, 545, 620, 715, and 780°C for periods of about five days each. No significant nitrogen permeation has been observed; the effective sensitivity of the instrument is such that a flow of about 10^{-6} Torr-cm^3/sec-cm^2 could have been detected. Using the permeation value of nitrogen through iron at 780°C, a flow of 10^{-2} Torr-cm^3/sec-cm^2 is calculated for the diffusion cell; the time to reach equilibrium is a few minutes. Either nitrogen permeation through stainless steel is much less than through iron (by a factor greater than 10,000) or the light oxide coating formed on the diffusion cell when it was inadvertently exposed to air while at temperature is a very good barrier to N_2 diffusion.

A new diffusion cell has been installed in the experiment. This cell is similar to the last cell; i.e., stainless steel tubing 1/8-in. o.d., 4-mil wall, and 40 in. long. The experiments will now be repeated.

C. Study of Soluble Getters in Sodium
(D. N. Rodgers, J. C. Biery)

1. General

For large sodium-cooled reactor systems, it may be desirable to use soluble getters for control of oxygen and other dissolved impurities in lieu of the more conventional hot and cold trapping techniques. The soluble getters of interest occur in the sodium coolant either naturally, as an impurity (calcium), or are produced during reactor operation (as with magnesium). The techniques for the controlled additions of these getters, maintenance of fixed getter levels, and the selective removal of depleted getter metals and other impurities from dynamic sodium systems must be developed if their usefulness is to be evaluated. The significant chemical reactions occurring in a sodium system containing these soluble getters must be understood and controlled. This mode of purity control has the potential for effectively controlling not only oxygen, but also carbon, hydrogen, nitrogen, and possible metallic impurities.

2. Current Results

All experimental work has been terminated, and a final report is in preparation. A summary of the results obtained from the project were presented in the previous quarterly.[2]

D. Study of Sodium Leaks
(J. P. Brainard)

1. General

The correlation of sodium leak development with measured helium leak rates observed during acceptance testing provides information on the degree of component integrity which must be attained for safe, long-term sodium plant operation. No firm criteria now exist that establish acceptable levels of leak-tightness for various situations.

This study uses fabricated stainless steel leaks and leaks that occur naturally in stainless steel bar stock. Selected samples having a range of helium leak rates are incorporated into small sodium systems (cells) which are held at a predetermined temperature until sodium leakage occurs. From these observations it may be possible to establish, for mass spectrometer acceptance tests on sodium system components, the maximum tolerable helium rate which is consistent with adequate long-term containment of sodium by that component.

An interesting side effect from this work has been observation of the elusiveness of what are considered to be large leaks (10^{-5} to 10^{-6} atm cm^3/sec). Normal fabrication contaminants such as grease, water and some solvents can completely mask leaks of this size and invalidate a leak test, unless proper pretreatment of the component is performed; and in some cases this can involve firing of the component in a hydrogen atmosphere. If meaningful helium leak tests are to be performed on LMFBR components, procedures must be developed for treating and handling of the part prior to leak test.

2. Current Results

Cells 1, 2, and 3 remain leak tight after 14,750 h at 400°C. Cell 4 (400°C) has about the same leak rate (2×10^{-2} cm^3 of sodium per day) as reported last quarter; the rate is increasing slightly. The leak rate of Cell 8 (650°C) has decreased by nearly a factor of 100, and there was no loss of nitrogen gas in the reaction chamber as reported last quarter. It may be that a reaction

between the steel and nitrogen has formed a plug in the leak.

E. Development of a Remotely Operated Distillation Sampler for EBR-II
(E. O. Swickard, J. R. Phillips)

1. General

The original objective of the project was to produce three remotely-operated distillation samplers: one as a prototype, one for installation on the EBR-II primary loop, and one for installation on the EBR-II secondary. Because of program funding reductions, the objective has been curtailed to the production of the prototype unit only.

The sampler is an engineering loop version of a laboratory model in use on Sodium Analytical Loop No. 1 and Plugging Indicator Loop No. 2 at LASL. Samples are taken from a continuously flowing bypass stream. The sampler is fabricated from Type 304 stainless steel, and energy for sodium evaporation is supplied by induction heating.

2. Current Results

Preparations are being made to test the internal RF coil in a mockup of the remote sampler on Analytical Loop No. 1. The envelope around the coil will contain a window to allow observation of the sodium ionization and arcing that might occur around the RF coil. The parts required for the mockup are nearly completed.

F. Analysis of Dynamic Cold Trap Performance
(J. C. Biery, W. W. Schertz, D. N. Rodgers)

1. General

In sodium coolant systems for future LMFBR's it will be necessary to use cold traps for removal and control of oxygen and other contaminants. These cold traps should be designed to handle adequately the impurity loads and to maintain the impurity concentration level below some specified upper limit. For economic reasons, cold traps must be as small and simple as possible, while still satisfying the design requirements.

Knowledge of the mechanism of impurity deposition in cold traps is necessary to reach the optimum design for a given sodium coolant system. The rate of mass transfer of impurity species to cold trap surfaces must be measured and the effect of various flow patterns, surface conditions, and temperature on the mass transfer rates must be determined. The purpose of this study is to determine the effect of the above variables on the mass transfer coefficient for removal of oxygen from sodium systems. Knowledge of the mechanisms involved and the mass transfer coefficients will allow calculation of the rate of oxygen removal and the location of deposited oxides in the cold trap for any given system size and cold trap geometry. Proposed cold trap designs could be evaluated in terms of total oxide capacity and expected system cleanup rates.

Cold trap tests are being conducted with a 60-gal sodium system which has analytical capabilities including a vacuum distillation sampler, a plugging indicator, and two UNC oxygen meters. The cold trap tests consist of measurement of the rates of change of oxygen concentration in the system. Various cold trapping conditions of temperature and flow rates are tested to determine the effect of these variables on the oxygen removal rates. When the rate of change of oxygen concentration, the cold trap temperatures and the deposition surface area is known an overall mass transfer coefficient can be calculated.

2. Current Results

Cold trap research in the Cold Trap Loop was terminated in October, 1969, after finishing a series of runs with the packed trap; the data have not been analyzed. An attempt to drain the trap and pull the removable core was made. The attempt failed because of sodium leakage through an isolation valve. As a result, the impurity deposits on the trap were dissolved off and lost. The loop is now being used in the plugging indicator studies.

Flushing of the gas space in the loop produced a large increase in impurity concentration in the loop. These deposits represented an impurity source that has not been taken into consideration in the cold trap calculations. Steady state runs at low cold trap temperatures have shown the influx of impurities from this source to be very small and probably not significant in the calculations of mass transfer coefficients. However, for similar type research where impurity balances are made, attempts should be made to remove deposits that accumulate above the gas-liquid interface.

V. REFERENCES

1. C. C. McPheeters and J. C. Biery, "The Dynamic Characteristics of a Na_2O Plugging Indicator," Nuclear Applications, 6, pp 573-81, June, 1969.

2. "Quarterly Status Report on Advanced Plutonium Fuels Program," July 1, to September 30, 1969, Report LA-4307-MS, Los Alamos Scientific Laboratory.

3. V. J. Rutkauskas, "Determination of the Solubility of Oxygen in Sodium Using the Vacuum Distillation Analytical Technique," Report LA-3879, Los Alamos Scientific Laboratory.

4. C. C. Addision, R. J. Pulham, and R. J. Roy, "Solutions of Hydrogen in Liquid Sodium," J. Chem. Soc. (London) pp 116-121, January 1965.

5. S. Kallmann and R. Liu, "The Determination of Total Carbon and Sodium Carbonate in Sodium Metal," Anal. Chem. 36, 590 (1964).

VI. PUBLICATIONS

1. J. P. Brainard, "Molecular Beams from Long Parallel Tubes," Report LA-4280-MS, Los Alamos Scientific Laboratory, December 4, 1969.

PROJECT 463

CERAMIC PLUTONIUM FUEL MATERIALS

Person in Charge: R.D. Baker

Principal Investigator: J.A. Leary

I. INTRODUCTION

The principal goals of this project are to prepare pure, well characterized plutonium fuel materials, and to determine their high temperature properties. Properties of interest are (1) thermal stability, (2) thermal expansion, (3) thermal conductivity, (4) phase relationships by differential thermal analysis, (5) structure and phase relationships by X-ray diffraction, high temperature X-ray diffraction, neutron diffraction and high-temperature neutron diffraction, (6) density, (7) hardness and its temperature dependence, (8) compatibility, including electron microprobe analysis, (9) compressive creep (deformation).

II. SYNTHESIS AND FABRICATION

(R. Honnell, S. McClanahan, H. Moore, R. Walker, C. Baker)

To meet the material needs of the physical property measurement program, a number of different carbide compositions were synthesized and fabricated into useful forms for testing. For E.M.F. measurements a 1.22 dia x 0.61 cm $PuC_{0.9}$ annuluses were sintered and characterized. For hot hardness and heat capacity determinations, cylinders of Pu_2C_3 measuring 2.45 dia x 0.92 cm and 1.22 dia x 0.92 cm were sintered and characterized. Compressive creep specimens measuring 1.22 dia x 1.10 cm were sintered from $(U_{0.8}Pu_{0.2})\,C_{1.0}$ powder.

The results from a cursory investigation on the effectiveness of nickel as a sintering aid for (U, Pu)C were reported previously, * except for identifying the chemistry of the metallic-appearing grain boundary precipitate. Microprobe analysis of the precipitate indicated that two phases were present containing predominantly plutonium and nickel with small amounts of uranium and little, if any, carbon. Uncorrected X-ray data indicated w/o compositions of 47 Pu - 34 Ni - 12 U and 60 Pu - 21 Ni - 12 U for these phases.

III. PROPERTIES

1. Differential Thermal Analysis

(J.G. Reavis, L. Reese)

Additional differential thermal analysis measurements have been made on Pu-C compositions. Results of Ta determination on Pu-C samples melted in carburized Ta containers are also reported. DTA observations of melting of UO_2 and UO_2-25% PuO_2 have been made to obtain base-line data for comparison with future observations of irradiated UO_2-25% PuO_2.

Observations of Pu-C Samples: Four Pu-C compositions in the range $PuC_{1.52}$ - $PuC_{2.00}$ have been investigated by DTA. All samples exhibited thermal arrests at 1660 ± 10°C. Liquidus temperatures were determined by heating the samples to selected temperatures,

*Quarterly Report on the Advanced Plutonium Fuel Program, July 1 to Sept. 30, 1969, Report LA-4307-MS, p 20.

quenching and examining visually to determine the extent of melting. The results are listed in Table 463-I. These values are in fair agreement with the currently accepted phase diagram of the Pu-C system.

Table 463-I

LIQUIDUS TEMPERATURES OF Pu-C SAMPLES

Composition	Liquidus, °C
$PuC_{1.52}$	2060 ± 10
$PuC_{1.58}$	2065 ± 10
$PuC_{1.78}$	2140 ± 20
$PuC_{2.00}$	2305 ± 20

The validity of liquidus temperatures determined in this way is dependent on the degree of dissolution of the carburized Ta containers. Results of analysis of some Pu-C samples for Ta after melting are given in Table 463-II. It appears that the concentrations of Ta in these samples are sufficiently low that liquidus temperatures would not be affected significantly, with the possible exception of the $PuC_{1.08}$ sample. A possible explanation of this high Ta concentration is that a chip of Ta could have inadvertently been included in the sample.

Table 463-II

Ta CONCENTRATIONS IN Pu-C SAMPLES AFTER MELTING

Composition	Ta Conc'n, w/o
$PuC_{1.08}$	5.5
$PuC_{1.25}$	0.6
$PuC_{1.32}$	< 0.02
$PuC_{1.45}$	0.6
$PuC_{1.78}$	0.3

Melting Behavior of Oxides: Samples of UO_2 and UO_2-25% PuO_2 have been melted in open W crucibles under 0.5 atm Ar. These experiments gave base-line data for comparison with similar experiments in the Wing 9 hot cells in which DTA of irradiated UO_2-25% PuO_2 is being done. UO_2 was observed to have a solidus temperature of 2830° and a liquidus of 2845°. The solidus of UO_2-25% PuO_2 was 2675° and the liquidus was 2775°.

2. Room Temperature X-ray Diffraction
(C.W. Bjorklund)

The characterization of plutonium ceramics by X-ray powder diffraction camera techniques has been included in other sections of this report. Studies of self-irradiation damage in plutonium compounds have been continued on a minimum-effort basis, i.e., samples are examined at approximately 6 month intervals to observe changes in lattice dimensions, quality of diffraction patterns, etc., with the following observations.

Oxides: PuO_2 enriched with 3.75% ^{238}Pu showed no deterioration in pattern quality over a 6-year period. The lattice dimension has been constant (saturated) for some time. Several reflections of unknown origin have been observed on the films for several years. Similar reflections have occasionally been observed on patterns of routine samples of $^{238}PuO_2$. Efforts to identify the source of the reflections have not been successful as yet.

Carbides: The lattice dimensions of both the two-phase PuC-Pu_2C_3 samples and the sample which was originally single phase (with the composition $PuC_{0.86}$) have been constant for some time. A second phase has grown into the latter sample characterized by weak, diffuse reflections at positions corresponding to those of Pu_2C_3. Additional reflections of unknown origin have appeared on films of this same material which could not be attributed to either Pu metal or Pu_3C_2. In particular, one reflection with an interplanar spacing of 3.02 Å has increased in intensity significantly on films of both the "single phase" ($PuC_{0.86}$) and two-phase (PuC-Pu_2C_3) samples in approximately two years. No further deterioration in the quality of the patterns has been observed.

In an earlier report, an equation was developed to express radiation damage in PuO_2 as a function of time and temperature. This equation, in turn, was used to calculate thermal annealing curves for PuO_2. In these equations, the lattice expansion was the physical property by which radiation damage was measured. Good agreement with experimental results was observed over the temperature range studied (75-675°K). This indicated that the observed lattice expansion of PuO_2 could be attributed to two opposing first order processes, the displacement of atoms to interstitial sites by self-

irradiation, and the thermal diffusion of defects (probably interstitial atoms) to randomly positioned sinks. Extrapolation to higher temperatures, however, was not successful, presumably because of the increased complexity of the annealing process. Attempts are currently underway to extend the applicable temperature range in order to more adequately describe the annealing behavior of radiation damaged PuO_2.

3. High Temperature X-ray Diffraction
(J.L. Green, K. Walters)

Investigation of the high temperature crystallographic properties of materials associated with the carbon-rich fields of the U-Pu-C phase diagram is continuing. Phase identification and thermal expansion data for the carbon-rich plutonium carbides have been reported previously. Studies of the mixed uranium-plutonium carbides were begun using material having an overall composition of $(U_{0.65}Pu_{0.35})C_{2.1}$. For this particular composition, thermal expansion data has been reported for the bcc sesquicarbide and for the fcc dicarbide. The details of phase identification for this mixed carbide have proven to be somewhat more complex than previous investigations have indicated; it is in this area that present studies are being carried out.

Several extraneous, low intensity reflections have been repeatedly observed at low angles throughout the temperature range of stability of $(U_{0.65}Pu_{0.35})_2C_3$, i.e., at temperatures below 1740°C. Two and occasionally three of these peaks have been present in almost every room temperature pattern recorded. Further, these lines were found to be stable toward annealing. It is often difficult to identify a phase from such an abbreviated line list; however, it has been possible to demonstrate that this pattern is due to the body centered tetragonal modification of the dicarbide. It was found that moderately rapid cooling from the fcc dicarbide phase field allowed significant amounts of the bct dicarbide to be quenched in. Patterns from these samples were complete enough to positively identify the quenched phase and to establish a correspondence between the three unidentified lines and the three lowest angle reflections in the bct pattern.

At higher temperatures, $1600°C < T < 1740°C$, the situation was somewhat different. Two unidentified, low intensity reflections have been repeatedly observed in this temperature region. The relative positions of these peaks are clearly not consistent with the bct pattern. Instead, they lie rather precisely on reflection positions predicted by extrapolation of high temperature lattice parameter data for the face centered cubic modification of the dicarbide. In addition, there is no observed tendency for the sesquicarbide phase to decompose or for the extraneous lines to increase in intensity, i.e., both phases appear to be stable at these temperatures.

In order to correlate these observations, the positions of all the low intensity peaks were determined as a function of temperature from 25°C to 1800°C. The interplanar spacings corresponding to the bct reflections expanded smoothly as a function of temperature up to 1500°C. At that temperature, the bct reflections disappeared and the "fcc" reflections appeared. On further heating, the interplanar spacings for these reflections joined smoothly with the high temperature data for the fcc dicarbide. This is regarded as sufficient to identify this phase as fcc dicarbide. Further study of the bct-fcc dicarbide transition at 1550°C indicates that the transformation is reasonably rapid and that it is reversible. Comparisons of peak heights for the fcc phases immediately above and below 1740°C indicate that approximately 8% of the dicarbide remains stable at the lower temperature.

At present, the only reasonable interpretation of these observations appears to be that two three-phase fields exist at this composition which have not previously been reported. Between 1740°C and 1550°C the phases observed are the body centered cubic sesquicarbide, graphite and a small amount of the face centered cubic dicarbide. The field beginning at 1550°C and having an undefined lower boundary contains the sesquicarbide, graphite and a small amount of the body centered tetragonal modification of the dicarbide.

4. Thermodynamic Properties of Plutonium Compounds by Electromotive Force Techniques
(G.M. Campbell)

The development of a galvanostatic method to measure equilibrium potentials has made it possible to use isotype electrodes in fused LiCl-KCl eutectic. This has had the unexpected result of extending the cell life of Pu containing compounds almost indefinitely. The reason for this unexpected increase in stability is now known to result from an equilibrium involving both Pu^{3+} (dissolved) and Pu^{4+}(dissolved). Cells containing pure Pu metal cannot reach a true equilibrium because Pu^{4+} is reduced at the pure Pu electrode and oxidized at the Pu-compound electrode resulting in a net transfer of Pu from cathode to anode. Initial studies involving a PuN electrode and a pure Pu electrode were successful because cell life times were limited to 200 h or less, N_2 reacts with Pu to form PuN, and because the mixed potential involving Pu^{4+} is not much different from the potential expected with the single ion Pu^{3+} present. However Pu compounds which have stabilities differing significantly from PuN result in large displacement from the single ion potential.

In order to make thermodynamic calculations from the rest potentials it is necessary to have thermodynamic information about the Pu^{3+}-Pu^{4+} equilibrium. When equilibrated with a PuN electrode this equilibrium is of the form

$$PuN_{(s)} + 3\ Pu^{4+}_{(x_2,\ \text{dissolved})} = 4\ Pu^{3+}_{(x_1,\ \text{dissolved})} + 1/2\ N_2 \qquad (1)$$

Since the thermodynamic properties of PuN are known, the free energy change involved in the reaction

$$Pu_{(\ell)} + 3\ Pu^{4+}_{(x_2,\ \text{dissolved})} = 4\ Pu^{3+}_{(x_1,\ \text{dissolved})} \qquad (II)$$

can be determined from the galvanostatically determined emf of the cell containing isotype PuN electrodes. The results of this reveal that $PuCl_3$ and $PuCl_4$ form ideal solutions in LiCl-KCl at mole fractions near 0.01 and at temperatures between 910 and 1050°K. The rest potentials of the cell

$$Pu_{(\ell)} \,|\, PuCl_{3(x_1)},\ PuCl_{4(x_2)},\ \text{LiCl-KCl} \,|\, N_2, PuN \qquad (III)$$

and the calculated emf for the cell (where $x_t = x_1 + x_2$)

$$Pu_{(\ell)} \,|\, PuCl_{3(x_t)},\ PuCl_{4(x_{0.5}t)},\ \text{LiCl-KCl} \,|\, W \qquad (IV)$$

are given in Table 463-III. With a free energy of formation for PuN at these temperatures of

$$\Delta G^{o}_{(PuN)} = -72,950 + 23.0\ T\ \text{cal/mole} \qquad (V)$$

a point by point calculation of the free energy change in reaction II results in

$$\Delta G^{o}_{(II)} = -341,250 + 137.2\ T\ \text{cal/mole} \qquad (VI)$$

for the temperature range 910 to 1048°K. The initial concentration of $PuCl_3$ in this experiment was 0.01061 mole fraction. By transpiration measurements Benz[1] found for this temperature range

$$\Delta G_T = 37,700 - 28.3\ T\ \text{cal/mole} \qquad (VII)$$

for the reaction

$$PuCl_{3(s)} + 1/2\ Cl_2 = PuCl_{4(g)} \qquad (VIII)$$

Assuming an ideal solution, by combining eq VI and VII the free energy of formation of $PuCl_3$ (dissolved) is

$$\Delta G^{o}_{T} = -228,150 + 52.3\ T\ \text{cal/mole} \qquad (IX)$$

and for $PuCl_4$ (dissolved)

$$\Delta G^{o}_{T} = -190,450 + 24.0\ T\ \text{cal/mole} \qquad (X)$$

Rand[2] estimates for pure $PuCl_{3(s)}$

$$\Delta G^{o}_{T} = -228,500 + 51.7\ T\ \text{cal/mole} \qquad (XI)$$

for this same temperature range. At a lower temperature (776-832°K) $PuCl_3$ (dissolved) was found[3] to be

$$\Delta G^{o}_{T} = -224,000 + 46\ T\ \text{cal/mole} \qquad (XII)$$

These results indicate strongly that the activity coefficients of both $PuCl_3$ and $PuCl_4$ in an equilibrium

Table 463-III

POTENTIALS FROM CELL III AND CELL IV

Emf Cell III,[1] V	Temp., °K	N_2 Pressure, atm	Emf Cell IV Calculated, V
0.7443	918.4	0.7681	0.7939
0.7428	920.6	0.7679	0.7939
0.7359	940.8	0.7763	0.7837
0.7329	941.7	0.7716	0.7726
0.7299	953.3	0.7730	0.7730
0.7208	976.8	0.7703	0.7620
0.7167	992.2	0.7726	0.7619
0.7083	1013.7	0.7743	0.7512
0.7091	1015.1	0.7708	0.7559
0.6992	1031.0	0.7741	0.7331
0.6924	1048.2	0.7755	0.7241
0.7017	1027.6	0.7774	0.7394
0.7104	1008.0	0.7734	0.7535
0.7158	997.6	0.7737	0.7643
0.7224	976.9	0.7784	0.7681
0.7215	979.0	0.7707	0.7672
0.7292	959.7	0.7741	0.7772
0.7286	962.5	0.7679	0.7781
0.7336	946.7	0.7667	0.7813
0.7399	931.1	0.7639	0.7900
0.7493	908.5	0.7670	0.8037

(1) Corrected for thermal Emf

Table 463-IV

POTENTIALS FROM CELL XIII

Rest Potential, V	Temp., °K	Single Ion Potential, V
0.3368	1015.7	0.2168
0.3413	991.9	0.2186
0.3495	955.7	0.2232
0.3457	972.9	0.2212
0.3539	937.8	0.2259
0.3530	952.7	0.2273
0.3459	958.6	0.2189
0.3498	949.1	0.2224
0.3499	942.9	0.2215
0.3528	923.8	0.2220
0.3493	945.2	0.2211
0.3476	961.1	0.2216
0.3438	977.8	0.2195
0.3460	967.5	0.2206
0.3419	986.9	0.2186
0.3442	976.6	0.2198
0.3406	996.1	0.2185
0.3362	1008.3	0.2147
0.3356	1003.5	0.2131
0.3398	986.9	0.2158
0.3465	970.6	0.2218
0.3417	969.4	0.2152
0.3481	934.9	0.2177
0.3542	917.3	0.2227

mixture at these temperatures in LiCl-KCl eutectic are very nearly unity.

Studies of the cell

$$Pu_{(\ell)} \mid PuCl_{3(x_1)}, PuCl_{4(x_2)}, LiCl\text{-}KCl \mid Pu_2C_3 + C \qquad (XIII)$$

were also made over the temperature interval 917 - 1016°K. The results are given in Table 463-IV. The initial concentration of $PuCl_3$ was 0.00279. A least squares analysis of the rest potentials results in

$$E = 0.5349 - 0.0001960\ T\ V\ . \qquad (XIV)$$

A point by point calculation taking into account the change in concentrations due to disproportionation results in

$$E_{(Pu_2C_3)} = 0.30339 - 0.00008683\ T\ V \qquad (XV)$$

where $E_{(Pu_2C_3)}$ is the single ion potential. This gives

$$\Delta G^{o}_{T} = -42,000 + 12.0\ T \text{ cal/mole} \qquad (XVI)$$

for the free energy of formation of Pu_2C_3. This is in reasonable agreement with the extrapolated free energy values found by vapor pressure measurements[4,5] but differs in slope of free energy versus temperature.

A paper which presents the theoretical approach and method of calculation for these systems has been prepared for publication.

5. Mass Spectrometric Studies of the Vaporization of Pu Compounds
(R. A. Kent)

A. Calibration of Magnetic Mass Spectrometer

The optical windows of the new RM6-K magnetic mass spectrometer have been calibrated for use with an optical pyrometer. In addition, a series of vaporization experiments have been performed with a gold standard sample. The purpose of these experiments was to calibrate the instrument for vaporization experiments and to become familiar with the operation of the unit. These experiments were performed with the instrument in an "off the shelf" condition and the results indicate that we can use this unit to satisfactorily perform the types of experiments planned when the unit was purchased. However, as a result of these calibration experiments, certain modifications are planned which will both extend the range and increase the precision of the measurements.

A sample consisting of 0.5 g Au wire (99.999 percent pure) obtained from the NBS was contained in a graphite cup in a Mo Knudsen cell and effused over the range 1329-1698°K. The ion current of the $^{197}Au^{+}$ signal was monitored as a function of temperature in the usual manner. The resultant least-squares equation is

$$\log_{10}(IT) = (21.317 \pm) - 18041 \pm 177/T^{o}K. \qquad (1)$$

At 1553°K, $\log_{10} P_{Au}(atm) = -5.876$.[6] The value obtained for $\log_{10}(IT)$ at the same temperature is 9.719. Thus, from the relationship $P = K(IT)$, one obtains $K = 3.75 \times 10^{-16}$ atm/amp deg K. and eq (1) becomes

$$\log_{10} P_{Au}(atm) = 5.891 - 18041/T^{o}K. \qquad (2)$$

Equation (2) yields for the heat and entropy of vaporization at 1533°K the values 82.55 ± 0.81 kcal/mole and 26.96 ± 0.53 eu, respectively. Published thermodynamic functions for Au(ℓ)[7] and Au(g)[8] were employed to reduce these values to 298°K. The second law values obtained are $\Delta H^{o}_{V\,298} = 87.9 \pm 0.8$ kcal/mole and $\Delta S^{o}_{V\,298} = 31.9 \pm 0.5$ eu. The third law heat of vaporization is calculated to be 87.7 ± 0.3 kcal/mole. The values listed for the NBS standard gold reference

Table 463-V

VAPOR PRESSURE DATA FOR GOLD

Pt*	Temp., °K	P_{Au} (atm) (x 10^6)	$\Delta H^o_{v\,298}$ kcal/mole
A 1	1567	2.29	87.87
A 2	1623	6.11	87.65
A 3	1592	3.94	87.47
A 4	1588	3.40	87.73
A 5	1350	0.0357	87.57
A 6	1376	0.0661	87.48
A 7	1504	0.652	88.30
A 8	1526	1.00	88.22
A 9	1553	1.72	88.02
A 10	1533	1.28	87.86
A 11	1520	0.918	88.15
A 12	1520	0.918	88.15
A 13	1513	0.809	88.15
A 14	1513	0.832	88.07
A 15	1507	0.738	88.10
A 16	1507	0.738	88.10
A 17	1506	0.667	88.35
A 18	1378	0.0698	87.45
B 1	1468	0.420	87.60
B 2	1514	0.805	88.22
B 3	1583	3.24	87.62
B 4	1611	5.06	87.65
B 5	1592	3.75	87.62
B 6	1561	2.19	87.83
B 7	1557	2.14	87.55
B 8	1530	1.20	87.89
B 9	1608	4.99	87.54
B 10	1616	5.28	87.76
B 11	1638	7.53	87.73
B 12	1638	7.50	87.75
B 13	1638	9.14	87.10
B 14	1575	3.33	87.11
B 15	1641	9.53	87.12
B 16	1645	10.2	87.11
B 17	1665	11.3	87.75
B 18	1698	17.3	87.94
B 19	1692	14.4	88.27
B 20	1626	5.89	87.92
B 21	1582	3.35	87.46
B 22	1583	3.22	87.64
B 23	1526	1.21	87.65
C 1	1515	1.03	87.54
C 2	1541	1.46	87.88
C 3	1529	1.18	87.88
C 4	1504	0.840	87.55
C 5	1472	0.509	87.26
C 6	1472	0.496	87.34
C 7	1501	0.820	87.45
C 8	1457	0.342	87.58
C 9	1421	0.137	88.12
C 10	1421	0.129	88.28
C 11	1389	0.0791	87.76
C 12	1329	0.0244	87.27
			Av = 87.74 ± 0.34

*Data for runs B and C were normalized for changes in multiplier gain from that for run A.

material are $\Delta H^o_{v\,298}$ = 87.7 kcal/mole and $\Delta S^o_{v\,298}$ = 31.8 eu. The vapor pressure data for the reaction Au(ℓ) = Au(g), together with the third law heat values, are listed in Table 463-V.

B. Planned Modifications

1. The 10-stage electron multiplier with a gain of about 3 x 10^4 will be replaced with a recently purchased 16-stage unit having a gain of about 10^6.
2. A new shutter slit will be installed to provide for sharper peak profiles.
3. The ion source exit slit will be enlarged to increase sensitivity.
4. The Hitachi ion gauges will be replaced with standard Bayard-Alpert gauges.
5. The Giessler discharge tubes used during preliminary pumping will be replaced with standard U.S. thermocouple gauges.
6. The ion source is being modified to allow RPD measurements.
7. The enclosure assembly which will allow us to operate with plutonium-containing samples, is being designed.

C. Other

A series of Pu-C samples have been prepared. These samples have the following stoichiometries: $PuC_{1.26}$, $PuC_{1.52}$, $PuC_{1.58}$, $PuC_{1.78}$, and $PuC_{2.00}$. Experiments using these samples will be performed in the new mass spectrometer.

6. High Temperature Calorimetry
(A. E. Ogard)

The vacuum isoperibal drop calorimeter described in the last report has been used for the determination of the high temperature heat content of Al_2O_3 and PuO_2.

Figure 463-1 is a plot of the present results on Al_2O_3 along with the results of P. B. Kantor et al.,[9] A. E. Ogard and J. A. Leary[10], and A. C. Macloed.[11] The present results can be expressed by the equation

$$H_T - H_{298} = -10.26 + 2.600 \times 10^{-2} T + 1.439 \times 10^{-6} T^2 + 7.091 \times 10^2 / T, \text{ kcal/mole}$$

over the temperature range 1350 to 2320°K, where T is in °K. This equation was obtained by a computer least squares fitting of the data with the restrictions that

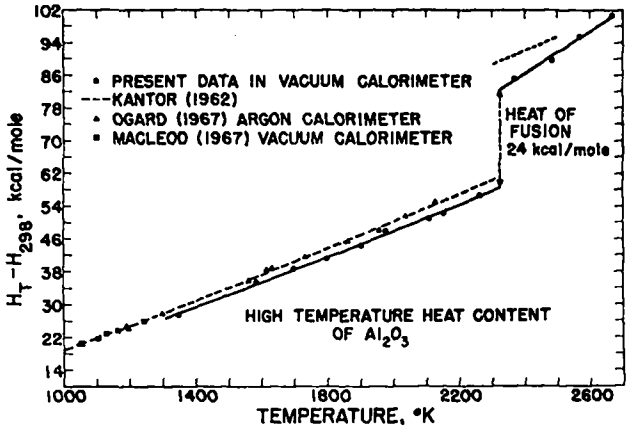

Figure 463-1. High Temperature Heat Content of Al_2O_3

$H_T-H_{298} \approx 0$ at T = 298°K and that $C_{p\,(298)}$ = 18.44 cal/mole/deg. These new results are from 2-4% lower than previous results in the range 1350-2265°K. In both sets of experiments the sample and the calorimeter were the same except Ar was used in the calorimeter in the earlier set and vacuum in the last set of experiments. This change in atmosphere in the calorimeter greatly affects the method of heat leak of the calorimeter, the constancy of the cooling rate of the calorimeter and the calibration factor of the calorimeter. A more detailed report of these results is in preparation. These results point out that high temperature heat contents are accurate to about ± 1% and that heat capacities obtained by differentiation of the heat content equation are estimated to be no better than ± 5% in accuracy. These limits of accuracy must be kept in mind when high temperature heat contents and heat capacities are used in other calculations.

The heat of fusion of Al_2O_3 of 24 kcal/mole measured from Fig. 463-1 is lower than the 28.3 kcal/mole reported by P. B. Kantor et al.

The high temperature heat content of PuO_2 has been determined from 1500 to 2715°K in the vacuum isoperibol drop calorimeter. The results shown in Fig. 463-2 can be expressed by the equation

$$H_T-H_{298} = -4.947 + 1.531\times10^{-2}T + 2.644\times10^{-6}T^2 + 43.61/T,\ \text{kcal/mole}$$

for the temperature range 1500-2400°K. Above 2400°K defect formation or some other phenomena causes a positive deviation from the equation. This equation was

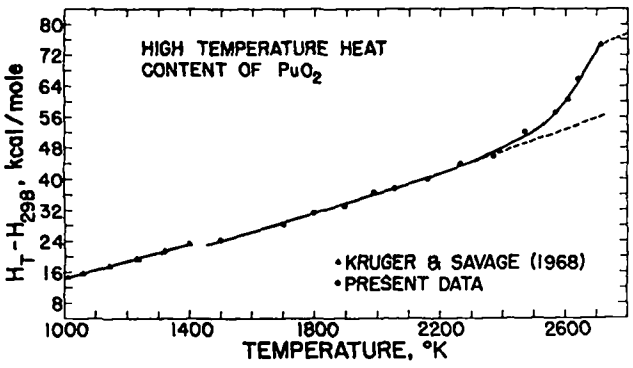

Figure 463-2. High Temperature Heat Content of PuO_2

determined by a computer least squares fit of the data with the restrictions that H_T-H_{298} = 0 at T = 298°K and $C_{p(298)}$ = 16.4 cal/mole/deg. These results are lower than expected from an extrapolation of the results of O. L. Kruger and H. Savage[12] but consistent with the difference between results obtained in an inert gas filled calorimeter versus a vacuum calorimeter.

The heat of fusion of PuO_2 can be estimated from the difference of heat content of molten PuO_2 and an extrapolation of the heat content equation to the melting point. A value of 18 kcal/mole is calculated for the heat of fusion of PuO_2. An X-ray radiograph of the sample after heating to 2715°K showed that the PuO_2 had been molten.

7. Transport Properties
(K. W. R. Johnson and J. F. Kerrisk)

A. Electrical Resistivity

Wiring of the electrical equipment for electrical resistivity measurements of samples outside a glove box at room temperature is complete. Resistivity measurements have been made on a number of standard materials at room temperature (23° to 25°C). The samples were right circular cylinders varying from 1/4 inch to 1/2 inch in diameter and 1/2 inch to 2 inches long. A jig for holding samples in this size range was also constructed. The results of the resistivity measurements are shown in Table 463-VI.

Table 463-VI
ROOM TEMPERATURE ELECTRICAL RESISTIVITY

Material	Resistivity, μ Ω cm
Inconel 702	124
Alloy A-286	95
Armco Iron	10.6
Tungsten	5.7
Molybdenum	5.6

The high temperature furnace for electrical resistivity measurements has been delayed. Delivery is not expected until March 1970.

B. Thermal Diffusivity

Preliminary tests on the Korad K-2 laser system were carried out to examine the pulse shape and duration, and the energy output of the laser. The pulse duration of approximately 1/2 m sec is short enough to be considered instantaneous for most materials; thus no correction for pulse duration will be required. The energy output as a function of capacitance and voltage was also determined. During these tests the energy output (at constant capacitance and voltage) decreased by approximately 40%. Subsequent disassembly of the laser head indicated that the aluminum flash lamp reflector was coated, reducing its reflectivity. Some scale was also found in the laser head cooling water system. A new pump and filter have been ordered for the cooling water system.

Preliminary measurements of the thermal diffusivity of Armco Iron, alloy A-286, and type 304 stainless steel have been made at room temperature. The results are shown in Table 463-VII. The measurements were made with a temporary sample holder, and a thermocouple was used to detect the temperature change.

Table 463-VII

ROOM TEMPERATURE THERMAL DIFFUSIVITY

Material	Thermal Diffusivity, cm^2/sec
Armco Iron[(a)]	0.194 to 0.223
304 Stainless Steel	0.0385 to 0.0395
Alloy A-286	0.0322 to 0.0337

(a) Data were taken on 4 samples of different thickness and from different sources.

Performance tests were run on the Centorr high temperature furnace in Suncook, N.H. At that time the power supply AC ripple was slightly above specification, but the manufacturer subsequently modified the power supply to meet the specification. The unit has been shipped.

C. Thermal Conductivity

Thermal conductivity values were calculated from the thermal diffusivity measurements of ANL - 75% dense and MLM - 91% dense $U_{0.8}Pu_{0.2}C$. These values were compared with thermal conductivity values calculated from the previously reported equation based on LASL data:

$$K_P = (0.0394 + 2.53 \times 10^{-5} T)\left(\frac{1-P}{1+4.01P}\right)$$

where K_P = Thermal Conductivity of Porous Material

T = Temperature, ^{o}C

P = Pore Fraction

The correlation from ANL-75% dense material was extremely close, varying ± 6% over the temperature range 400-1000°C. Over the same temperature range values calculated from the MLM - 91% dense diffusivity measurements were 20-42% lower than values calculated from the above equation. This decrease may be attributed to the presence of significant quantities of sesquicarbide and oxide which were present in the MLM specimens.

8. Mechanical Properties
(M. Tokar, A. Gonzales)

Hot hardness tests were conducted on various uranium-plutonium carbide compositions, using an apparatus described previously. Hardness indentations were made with a diamond or sapphire indentor at temperatures up to 1000°C in vacuum. The common load was 200 g. After the indentations had been made and the specimen cooled, it was transferred out of the glovebox to a standard Leitz hardness tester where the indentations were then measured.

Hot hardness curves for some of the carbide compositions which have been tested to date are shown in Figure 463-3. All of the curves are for sintered material. Curves 5 and 6 for UC and curve 7 for $U_{0.85}Pu_{0.15}C$ were taken from the literature[13] and are shown for comparison. Each data point for curves 1-4 represents the mean value of a minimum of 5 readings.

Curve 1 shows the hot hardness behavior of a PuC specimen containing about 10 v/o Pu_2C_3. As shown, up to about 500°C, this material had a hardness comparable to the mixed carbides, and was in fact harder than the literature values for UC or $U_{0.85}Pu_{0.15}C$, but above 500°C the hardness dropped rapidly.

The hot hardness behavior of a hypostoichiometric

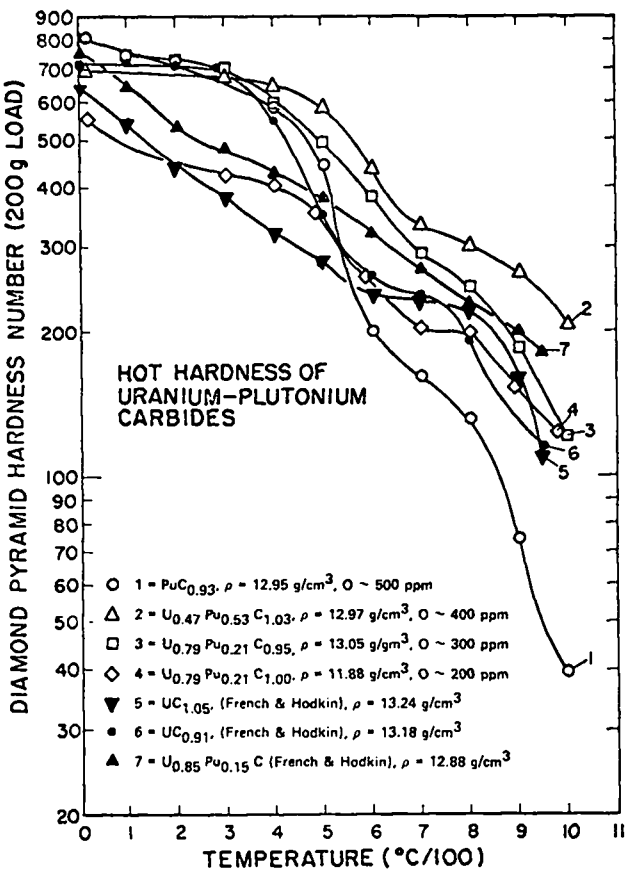

Figure 463-3

specimen of PuC containing some Pu_3C_2 has also been determined but is not shown in this figure. This material had a diamond pyramid hardness of about 270 at room temperature, dropping to 36 at 550°C.

That some solid solution strengthening is obtained from the addition of PuC to UC is evident from a comparison of the curves for UC with those of the mixed carbides. The highest hardness values at high temperatures were obtained for specimen 2 which contained about a 1:1 mole ratio of Pu to U.

The hot hardness behavior of PuN, UN,[14] and $U_{0.7}Pu_{0.3}N$[13] are shown in Fig. 463-4. At low temperatures the nitrides are considerably softer than the carbides. Comparing PuN with PuC, however, at temperatures above 800°C PuN is harder than PuC. It can be seen from this figure that a strengthening or hardening effect is obtained from alloying UN with PuN, since the PuN-UN solid solution is harder than either component alone. Future work will include the further investigation of the effects of stoichiometry and U/Pu

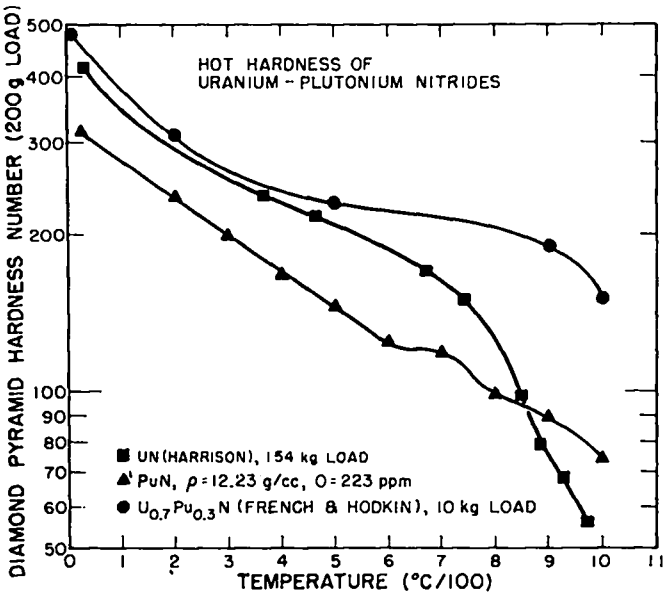

Figure 463-4

ratio on the hot hardness of the monocarbides as well as measurements of the hot hardness of compounds which have not been tested heretofore such as the sesquicarbides.

IV. ANALYTICAL CHEMISTRY

1. Determination of O_2 in Refractory Oxides, Carbides, and Nitrides

(M. E. Smith and J. E. Wilson)

Modifications are being investigated to improve the analyses of ceramic-type materials for O_2 because of the great effects caused by this element on the properties of refractory oxides, carbides, and nitrides. One modification is the use of a microwave excited emissive detector system to measure the O_2 evolved as CO from the sample as it is inductively heated to 2000°C in a graphite crucible. A known fraction of the CO is swept by Ar through a microwave-excited discharge cell which is monitored photometrically, and the O_2 concentration is calculated from the time-integrated signal from the photometer. Fifteen analyses each of U_3O_8 and ZrO_2, used as stand-in materials for oxide fuels, showed that the relative standard deviation (1σ) of the method was 1.8%, and the average bias was less than 0.25 relative percent. This precision is better than the 10 relative percent of the capillary trap-micromanometric measurement of O_2,[15] but not as good as the 0.2 relative percent of the inert gas fusion-

gravimetric method.[16]

Small changes in several operating conditions were tried to improve the precision of the analyses. Variations in the fraction of CO passed through the excitation cell, and in the wall temperature, discharge background, and exit gas pressure of the excitation cell did not improve the reproducibility of the measurements significantly. Addition of graphite powder to the sample crucible offered promise of improving the precision, and additional tests of this change were started.

A second modification being investigated was substitution of impulse heating for induction heating of the sample. In the impulse heater fabricated at LASL, the sample in a covered graphite crucible was rapidly heated to a temperature between 3000°C and 3400°C by a large direct current of short duration. The O_2 in the sample was evolved as CO, trapped on SiO_2 gel cooled with liquid N_2, and then measured on a gas chromatograph. The gas chromatographic measurements were reproducible within 4 relative percent. Initial tests of the complete apparatus by analyzing four prepared U_3O_8-TaC mixtures, each weighing about 5 mg, indicated that the estimated relative standard deviation of the method was about 10 percent. Refinements in the operations, especially in transferring the collected CO to the gas chromatograph, were being tested to improve the precision.

V. REFERENCES

(1) R. Benz, J. Inorg. Nucl. Chem., 24, 1191(1962).

(2) M.H. Rand, IAEA 4, Special Issue No. 1 Plutonium, Vienna (1966).

(3) G.M. Campbell, L.J. Mullins, and J.A. Leary, "Thermodynamics of Nuclear Materials, 1967," IAEA, Vienna, 75 (1968).

(4) W.M. Olson and R.N.R. Mulford, "Thermodynamics of Nuclear Materials, 1967", IAEA, Vienna (1968).

(5) R.A. Kent, "Mass Spectrometric Studies of Plutonium Compounds at High Temperatures. The Plutonium-Carbon System," Int. Conf. on Mass Spec., Kyoto, Japan, Sept. 8-12, 1969.

(6) U.S. National Bureau of Standards, Gold Standard Reference Material 745.

(7) J.W. Tester, R.C. Feber, and C.C. Herrick, J. Chem. Eng. Data 13, 419 (1968).

(8) R. Hultgren, R.L. Orr, P.D. Anderson, and K.K. Kelley, Selected Values of Thermodynamic Properties of Metals and Alloys, J. Wiley and Sons, Inc., New York, N.Y., 1963.

(9) D.B. Kantor et al., Ukr. Fiz. Zh., 7, 205 (1962).

(10) A.E. Ogard and J.A. Leary, "Thermodynamics of Nuclear Materials, 1967," IAEA, Vienna (1967).

(11) A.C. Macloed, Trans. Far. Soc., 63, 300 (1967).

(12) O.L. Kruger and H. Savage, J. Chem. Phy., 49, 4540 (1968).

(13) P.M. French and D.J. Hodkin, "Mechanical Properties and Compatibility of Uranium-Plutonium Carbides," Plutonium 1965, Inst. Metals, London, Chapman and Hall, pp 697-720 (1967).

(14) J.D.L. Harrison, "The Hot Hardness of Uranium Carbonitrides," Fuels and Materials Development Program Quarterly Progress Report for Period Ending June 30, 1968, ORNL-4330, D.J. Rucker, Ed., November 1968.

(15) W.G. Smiley, Anal. Chem., 27, 1098 (1955).

(16) C.S. MacDougall, M.E. Smith, and G.R. Waterbury, Anal. Chem., 41, 372 (1969).

VI. PUBLICATIONS

1. "The Thermal Conductivity of Uranium-Plutonium Carbides," K.W.R. Johnson and J.A. Leary, presented at American Nuclear Society Winter Meeting, San Francisco, Nov. 30 - Dec. 4, 1969.

2. "Mechanical Properties of Carbide and Nitride Reactor Fuels," M. Tokar, A.W. Nutt, and J. A. Leary, Ibid.

3. "Synthesis and Fabrication of Carbide Fuels," J.A. Leary, M.W. Shupe, R. Honnell, and A.E. Ogard, Ibid.

4. "Differential Thermal Analysis Apparatus for Observation of Refactory Plutonium Compounds," J.G. Reavis, J.F. Buchen, and J.A. Leary, Los Alamos Scientific Laboratory Report No. LA-4103 (1969).

PROJECT 464

STUDIES OF Na-BONDED (U,Pu)C LMFBR FUELS

Person in Charge: D. B. Hall
Principal Investigator: R. H. Perkins

I. INTRODUCTION

The use of a sodium bond between (U,Pu)C fuel and the clad in an LMFBR fuel element is being investigated at LASL. The high thermal conductivities of both the fuel and the sodium bond should permit the fuel elements to operate at high linear heat ratings. Space originally occupied by the sodium bond is available to accommodate fuel swelling during burnup.

An object of concern in the utilization of carbide fuel is its compatibility with cladding materials. The mechanism and kinetics of carbon transfer through a sodium bond to Type 316 stainless steel and to refractory metal claddings are being investigated. The effects of significant fuel and sodium variables (such as oxygen content) on this carbon transfer are being studied.

The performance limitations of the sodium bond under high-heat-flux conditions are being determined both in-pile and out-of-pile. The effects of defects in the sodium bond, and the resultant perturbation in heat transfer, are being studied utilizing a central high-heat-flux heater.

Another part of the program is concerned with the behavior of defected fuel elements in high velocity sodium. These studies are concerned principally with the "washout" of fuel from the defected element and the movement of this fuel in the sodium system. The determination of the solubility of uranium and plutonium in sodium is necessary to set upper limits on the loss of fuel to the sodium coolant.

High purity single-phase $(U_{0.8}Pu_{0.2})C$ is the principal fuel used in these investigations. Fuel loading and testing are done under carefully controlled conditions. Information obtained in this program, together with irradiation performance data (Project 467), will be used to evaluate sodium-bonded (U,Pu)C fuel for LMFBR application.

II. SYNTHESIS AND FABRICATION OF FUEL PELLETS (R. Honnell, S. McClanahan, R. Walker, G. Moore, C. Baker)

A. General

Standardized procedures for producing single-phase monocarbide pellets of known composition and dimensions have been developed. These pellets will be utilized in EBR-II irradiation experiments and compatibility testing. Basic process steps are:

1. Multiple arc melting of a 60-g mixture of ^{235}U, Pu, and C using a graphite electrode.
2. Solution treatment of the arc melted ingot for 24 h at 1600°C.
3. Crushing and grinding of the ingot in a WC vibratory mill, followed by screening of the resulting powder to a particle size range $\leq$ 62 μ.
4. Elimination of higher carbides by reaction with H_2 at 850°C.
5. Cold compaction at 10 tsi into pellets without the use of binders or sintering aids.
6. Sintering the pellets in Ar at 1800°C for 8 h followed by heat treatment for 2 h at 1400°C.
7. Characterization of the pellets by linear dimensioning, weighing, x-ray diffraction analysis, chemical analysis for U, Pu, C, N, O, and trace impurities, radiography for

determination of possible internal cracks, and isotopic analysis of uranium and plutonium.

B. Current Results

Characterization results from randomly sampled pellets representing nine (U,Pu)C lots prepared using the above process are listed in Tables 464-I to 464-IV. Metallographic results indicate that all of the pellets are single phase except those from lot HNL 8-62-1 which contain a grain boundary phase estimated at less than 0.5 v/o. The chemistry of this minor phase was not established, but in appearance it is identical to a plutonium-rich phase containing varying amounts of silicon, iron, and tungsten identified in similar (U,Pu)C pellets.

Approximately 75 pellets with a nominal composition of $(U_{0.8}Pu_{0.2})C_{1.0}$ have been fabricated from uranium-233 and are being characterized. Metallographic results show that these pellets contain a grain boundary phase of 0.5 v/o or less. Again, this grain boundary phase is similar in appearance to that seen previously in other (U,Pu)C pellets. This is probably a plutonium-silicon combination, since the silicon content of the U-233 metal used in alloying was three to four times that of the U-235 normally used. Microprobe analysis is pending.

To minimize chipping during fuel pin loading, pellets are being pressed with top and bottom die punches machined to leave a 45° chamfer on the pellet ends. Although this technique readily produces a chamfer on the sintered pellets, it also apparently increases the probability of end capping, i.e., a concave microcrack across the pellet edge penetrating to a depth of 200 to 400 microns. Of the 60 chamfered pellets prepared, 24 have failed to pass inspection because of end caps. This is a higher number of rejections than would be expected from the same number of nonchamfered pellets.

Table 464-I

CHEMICAL COMPOSITION AND PROPERTIES OF (U,Pu)C LOTS

	Nominal, w/o			Analyzed, w/o			Immersion Density
Lot Number	U	Pu	C	U	Pu	C	(g/cm^3)
HNL 8-8-1	75.9	19.25	4.84	76.4	18.39	4.72	12.95
HNL 8-8-2	75.9	19.28	4.84	76.6	18.36	4.66	12.72
HNL 8-10-1	75.8	19.31	4.84	76.3	18.74	4.71	12.95
HNL 8-10-2	75.9	19.27	4.84	76.4	18.21	4.71	13.11
HNL 8-16-1	76.1	19.13	4.79	76.9	18.26	4.64	13.13
HNL 8-16-2	75.8	19.30	4.84	75.6	18.73	4.72	12.94
HNL 8-18-1	75.8	19.30	4.84	76.5	18.75	4.73	12.78
HNL 8-18-2	75.9	19.29	4.84	76.4	18.47	4.63	12.98
HNL 8-62-1	74.9	20.2	4.84	75.3	19.67	4.65	12.76

Table 464-II

IMPURITY CONTENTS OF PELLETS (ppm BY WEIGHT)

Lot Number	O	N	Zn	Na	Si	Ca	V	Cr	Fe	Cu	Mo	W	Ni
HNL 8-8-1	240,510,460**	310	*	*	40	*	5	*	35	*	*	25	*
HNL 8-8-2	760,510,360	330	*	*	45	5	5	15	110	10	*	10	*
HNL-8-10-1	290,870,1100	280	*	*	25	*	5	*	70	10	*	*	*
HNL 8-10-2	410,360,510	720	*	*	35	*	5	*	45	5	10	*	*
HNL 8-16-1	280,430,660	270	*	*	70	*	5	*	65	10	10	*	10
HNL 8-16-2	590,830	270	*	2	35	*	5	20	95	15	10	*	10
HNL 8-18-1	370,380,400	305	*	*	45	*	5	15	90	20	10	*	10
HNL 8-18-2	320,350,640	340	*	*	50	*	5	25	110	20	*	10	10
HNL 8-62-1	420,340,360	225	20	*	*	*	*	*	15	*	25	10	*

*Below detectable limits.

**Three values for each lot.

Table 464-III

ISOTOPIC ANALYSES OF (U,Pu)C PELLETS

Lot Number	Pu, w/o						U, w/o				
	238	239	240	241	242	244	233	234	235	236	238
HNL 8-8-1	< 0.022	94.45	5.25	0.281	0.015	< 0.0005	< 0.0005	0.940	92.75	0.241	6.07
HNL 8-8-2	< 0.022	94.44	5.26	0.282	0.014	"	"	0.926	91.22	0.236	7.62
HNL 8-10-1	< 0.4	94.46	5.24	0.281	0.015	"	"	0.942	92.42	0.240	5.88
HNL 8-10-2	< 0.06	94.42	5.28	0.286	0.015	"	"	0.944	93.0	0.241	5.81
HNL 8-16-1	< 0.07	94.44	5.26	0.283	0.015	"	"	0.860	85.07	0.221	13.85
HNL 8-16-2	≤ 0.010	94.45	5.25	0.281	0.015	"	"	0.930	91.80	0.240	7.03
HNL 8-18-1	< 0.08	94.43	5.26	0.283	0.024	"	"	0.940	92.77	0.241	6.05
HNL 8-18-2	< 0.018	94.44	5.26	0.282	0.016	"	"	0.945	92.98	0.240	5.83
HNL 8-62-1	< 2.0	94.27	5.38	0.331	0.017	"	"	0.936	92.07	0.237	6.76

Table 464-IV

LATTICE PARAMETERS OF (U,Pu)C LOTS (Å)

Lot Number	a_o
HNL 8-8-1	4.9617
HNL 8-8-2	4.9622
HNL 8-10-1	4.9633
HNL 8-10-2	4.9631
HNL 8-16-1	4.9634
HNL 8-16-2	4.9642
HNL 8-18-1	4.9636
HNL 8-18-2	4.9634
HNL 8-62-1	4.9626

III. LOADING FACILITY FOR TEST CAPSULES
(D. N. Dunning, J. O. Barner, J. A. Bridge)

A. General

A prerequisite to a compatibility program involving (U,Pu)C and sodium is a satisfactory capsule loading and bonding facility. There is little point to obtaining well-characterized materials for testing if these materials are subject to contamination by impurities before they are placed in test. Sodium and (U,Pu)C are sufficiently reactive that all operations must be performed either in vacuum or in a high quality inert atmosphere. The loading facility for handling these materials has been constructed and is operational. The facility consists of inert-atmosphere gloveboxes equipped with inert-gas cleanup systems to provide an environment for handling fuel pellets and bonding sodium with a minimum of contamination.

B. Current Results

During this reporting period, EBR-II irradiation test capsules K-43 and K-44 containing 95% dense (U,Pu)C pellets were loaded and bonded. A modified bonding procedure appears to be satisfactory; problems with sodium bonding and pellet chipping in previous EBR-II irradiation test capsules were not encountered in these capsules. This new bonding procedure, which will be used on all future irradiation test capsules, is:

1. Place the loaded and sealed capsule in the centrifuge and heat, impressing an axial temperature gradient along the 14-1/2-in. fuel stack (150°C at the bottom and 280°C at the top).
2. Cool to room temperature while spinning at 150 rpm.
3. Heat the capsule to 600°C for 1 h and then cool to room temperature. Maintain a temperature gradient during heating and cooling so that the sodium melts from the top down and freezes from the bottom up.
4. Repeat Steps 1 and 2.

The sensitivity of the eddy-current tests for sodium bond defects is such that a 0.020-in. defect can be detected. Capsules K-43 and K-44 had no detectable defects in the sodium bonds in either the inner fuel pins or the outer capsules. These capsules are now ready for shipment to EBR-II.

Approximately 75 capsules for out-of-pile compatibility testing and OWR (Omega West Reactor) experiments were loaded and bonded during this quarter.

IV. CARBIDE FUEL COMPATIBILITY STUDIES
(F. B. Litton, H. A. O'Brien, L. A. Geoffrion)

A. General

The objectives of this program are to study the interactions among single-phase mixed uranium-plutonium carbide, a sodium bond, and potential

cladding materials, i.e., to investigate the technology related to sodium-bonded fuel elements. There are two approaches to the experimental work. The primary approach is to determine the reactions occurring between single-phase $(U_{0.8}Pu_{0.2})C$ and potential cladding materials, using Type 316 stainless steel and a high strength vanadium-base alloy as the first and second choices of cladding material, respectively. (The experimental work on high strength vanadium-base alloys is being de-emphasized.) The secondary approach is to study the mechanism of carbon transport through sodium, the effect of impurities such as oxygen, and the carburizing potential of fuel in contact with sodium and cladding materials.

Capsules containing sodium-bonded, single-phase (U,Pu)C are tested in sodium loops at temperatures from 450 to 750°C for periods up to 10,000 h. High purity, thoroughly-characterized sodium is used for the studies. Fuels of known composition are used in the tests. Most of the testing is performed on single-phase (U,Pu)C fuel in which the Pu/U ratio is maintained at 0.20, but some experiments are being carried out on material containing a second phase (either metallic or carbon-rich). Of particular interest is mixed carbide fuel containing ~ 10 v/o sesquicarbide. Other experiments employ stoichiometric and hyperstoichiometric UC to determine the effect of plutonium addition on the behavior of carbide fuel.

B. Current Results

1. Compatibility Studies with Mixed Carbide Fuels

Experiments are in progress to study the compatibility of sodium-bonded (a) single-phase mixed carbide fuel and (b) monocarbide plus ~ 10 v/o sesquicarbide fuel with Type 316 stainless steel and V-15Cr-5Ti alloy capsules. A 4000-h, 750°C-test of these two fuel types in Type 316 stainless steel capsules has been completed and preliminary information has been obtained from the examination of one capsule of the three that were tested with each fuel.

The LASL-prepared single-phase monocarbide fuel has a nominal composition of

$$(U_{0.796\pm0.001}Pu_{0.204\pm0.001})C_{0.97\pm0.01}O_{0.006\pm0.003}N_{0.005\pm0.001}H_{<0.001},$$

corresponding to 75.3 ± 0.4 w/o U, 19.57 ± 0.18 w/o Pu, and 4.70 ± 0.06 w/o C. The average chemical composition is based upon the analyses of 39 samples selected on a statistical basis. The average amounts of trace impurities are shown in Table 464-V. All pellets were x-ray radiographed and found to be free of any detectable cracks and chips. By x-ray analysis the material was found to be single-phase monocarbide with a lattice dimension of 4.965 ± 0.001 Å. The density is 89.8 ± 1.5% as determined by immersion and 89.0 ± 1.5% as determined by dimensional measurement. Metallographic examination showed a single-phase monocarbide microstructure. The grain size is generally < 55 and > 2 microns. A few inclusions were observed in some specimens; these are present to < 0.5 v/o as determined by point counting methods. The inclusions typically contain one or more of the following elements: Si, Fe, Ni, Cu, or W. In approximately 50% of the metallographic specimens examined, microcracks ~ 20 μm wide were observed. These microcracks appear as a necklace of interconnected porosity of short length, and are below the limit of detectability by radiographic examination. Although electron microprobe examination showed the pellets to be homogeneous on a macro- and intergranular scale, some heterogeneity in uranium and plutonium was observed

Table 464-V

SPECTROCHEMICAL ANALYSIS OF $U_{0.8}Pu_{0.2}C$ PELLETS

Element	ppm	Element	ppm
Li	< 1	Ni	19 ± 17
Be	< 1	Cu	40 ± 21
B	< 1	Zn	< 10
Na	< 2	Sr	< 5
Mg	< 5	Zr	< 100
Al	< 10	Nb	< 50
Si	57 ± 43	Mo	< 12
P	< 50	Cd	< 10
Ca	< 5	Sr	< 2
Ti	< 50	Ba	< 10
V	< 5	Ta	<1000
Cr	< 10	W	19 ± 18
Mn	3	Pb	< 2
Fe	55 ± 32	Bi	< 2
Co	< 5		

Note: Concentration of tantalum on a spot-check basis was < 25 ppm.

Table 464-VI

CHARACTERIZATION OF FUEL PELLETS RECEIVED FROM UNITED NUCLEAR CORPORATION

Carbon, w/o	4.79 ± 0.05*
Oxygen, ppm	3710 ± 50
Nitrogen, ppm	240 ± 20
Equivalent carbon content**, w/o	5.09
Plutonium, w/o	14.09 ± 0.06
Lattice dimensions, as determined by x-ray diffraction, Å	8.108 ± 0.002
Amount of $(U,Pu)_2C_3$, as determined by metallography, v/o***	10
Average pellet density, g/cm^3	13.15 ± 0.04
Average pellet diameter, in.	0.231 ± 0.001

*The variability shown was calculated at one standard deviation.

**The sum of C + 12/16 O + 12/14 N.

***The amount of phases was determined by point count and x-ray diffraction methods.

on an intragranular scale. No quantitative correlation between x-ray intensities and element concentration could be made, but the intensities varied by 10 to 20% for plutonium and by 20 to 30% for uranium.

The fuel pellets containing (U,Pu)C plus ~ 10 v/o $(U,Pu)_2C_3$ were processed by United Nuclear Corporation to its specification No. 16325 (issued Sept. 29, 1965, Rev. 3, Aug. 21, 1967). A characterization of the pellets is shown in Table 464-VI.

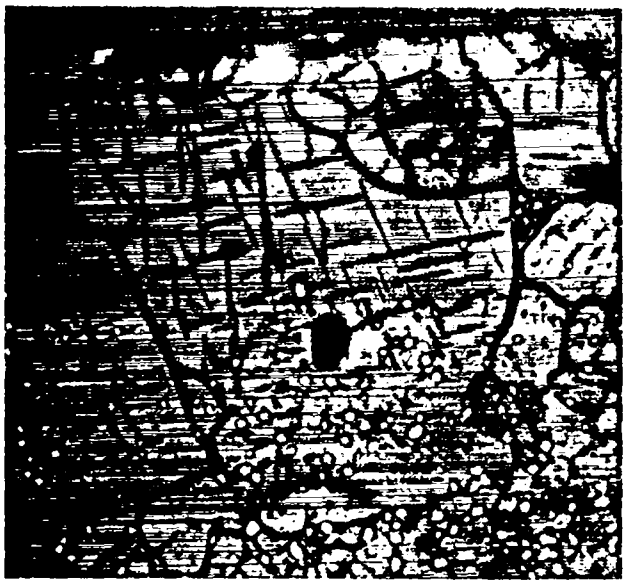

Fig. 464-1. A view of the surface of a UNC fuel pellet showing localized precipitate. Etched, 300X.

Autoradiography (United Nuclear Corporation) and electron microprobe analyses (LASL) both indicated homogeneity of microstructure. However, metallographic examination of a randomly selected pellet showed that the material consists of three phases; a monocarbide matrix, the sesquicarbide as the principal second phase, and trace amounts of an acicular phase (tentatively identified as the dicarbide). It should be pointed out that trace amounts of dicarbide are permitted under specification No. 16325. The localized acicular precipitate is shown in Fig. 464-1. The pellets had been surface ground at UNC to remove 0.006 in. from their diameter. They were degreased, degassed, and packaged under helium in stainless steel tubes with welded end-closure plugs. At the LASL, shipping tubes were opened, and the pellets were stored until encapsulation under purified helium.

For compatibility tests, three pellets and ~ 1 g of high purity sodium (< 10 ppm oxygen, < 10 ppm carbon) were loaded in 0.3-in.-o.d. by 0.280-in.-i.d. by 3-in.-long Type 316 stainless steel and V-15Cr-5Ti alloy capsules. Capsules were tested in triplicate by heating at 750°C in forced-convection, zirconium-gettered, Type 321 stainless steel sodium loops. After compatibility testing, the sodium bond was vacuum-distilled from the capsules at 500°C.

The examination of capsules heated for 4000 h at 750°C is in process. The metallographic study of one of the Type 316 stainless steel capsules containing each carbide type has been completed and results indicate that small amounts of carbon were transferred from both single-phase pellets and from those containing ~ 10 v/o of sesquicarbide. Relatively more carbon was absorbed by the Type 316 stainless steel cladding from the UNC pellets (~ 10 v/o sesquicarbide) than from the single-phase pellets. However, it is unlikely that the amount of carbon absorbed from either of the two pellet types was sufficient to affect drastically the physical properties of the cladding material.

The metallographic structure of the Type 316 stainless steel capsule containing UNC pellets showed sigma phase precipitation in areas not affected by carbon pickup. (The absorption of carbon and the subsequent precipitation of $Cr_{23}C_6$-type carbides removes chromium from the matrix, thus

reducing the tendency for sigma formation.) Figure 464-2 shows this sigma formation near the bottom closure weld. Negligible carbide precipitation occurred in this region. The typical structure along the capsule wall is shown in Fig. 464-3. In this region, carbide precipitation throughout the wall was observed. Some sigma phase was also present; the amount increased toward the outside wall of the capsule. A localized surface film, shown in Fig. 464-4, was observed only at the bottom of the capsule where the pellet was in contact with the stainless steel. This region showed general carbide precipitation and an insignificant amount of sigma formation.

Carburization of the Type 316 stainless steel capsule containing single-phase pellets occurred only in localized regions along the wall at the junction between pellets. Two carburized regions, approximately 1/4 in. from the bottom and from each other (corresponding to pellet height), were observed. One carburized region is shown in Fig. 464-5. The region showed general carbide precipitation accompanied by a reduction of sigma formation. A typical structure of the capsule wall away from the localized carburized regions is shown in Fig. 464-6. Sigma phase was uniformly distributed in the grain boundaries. Carbide precipitation occurred intragranularily in this region.

Examination of the single-phase fuel pellets revealed some intergranular attack; this is shown in Fig. 464-7. The pellets containing ~ 10 v/o $(U,Pu)_2C_3$ were attacked more extensively in regions generally associated with the presence of trace amounts of the acicular phase. This attack is shown in Fig. 464-8. It is significant that no sodium attack on the sesquicarbide phase in these pellets was observed. Figure 464-9 shows this unattacked sesquicarbide phase at the surface of a UNC pellet.

These preliminary data indicate that carbon absorption by the clad occurs from both types of fuel. Examination of the four additional capsules is in progress to test further the validity of these preliminary results. Previous tests (4000 h at 750°C) had indicated that no reaction occurred between sodium-bonded, single-phase, mixed-carbide fuel and Type 316 stainless steel capsules (LA-4073-MS, Jan. 9, 1969).

To determine the effect of oxygen content on compatibility of fuel containing sesquicarbide with cladding alloys, material containing ~ 10 v/o $(U,Pu)_2C_3$ was prepared at LASL. The LASL material contains 5.32-5.58 w/o C, 87-650 ppm N, and 350-850 ppm O. (Material prepared by UNC contains 4.8 w/o C, 240 ppm N, and 3700 ppm O.) These pellets were loaded into Type 316 stainless steel and vanadium alloy capsules, and the capsules have been placed in test at 750°C.

2. Compatibility Tests with Uranium Carbide Fuels

The experimental program to study the reaction of sodium-bonded $UC_{1.07}$ with Type 316 stainless steel was continued during this period. The structure of the carbide source consisted of a matrix of uranium monocarbide containing excess carbon as the sesquicarbide phase and trace amounts of the dicarbide phase. The program entails heating the carbide in Type 316 stainless steel capsules with sodium (~ 5 g) and a Type 316L stainless steel tab for 500 and 1000 h at 450, 550, 650, and 750°C.

The data obtained to date are summarized in Table 464-VII. Localized carburization of the capsule wall was observed metallographically only in the 1000-h, 550°C-test. This was in a region adjoining the $UC_{1.07}$ carbon source. Although metallographic examination did not show carburization of the other Type 316 stainless steel capsules, chemical analyses of the Type 316L test tabs indicated minor amounts of carbon pickup occurred in several cases. All the $UC_{1.07}$ carbon sources showed depletion of the dicarbide phase at the surface except in the capsule heated for 500 h at 450°C.

The dicarbide phase at the sodium contact surface appears to be the primary source of carbon for transport to the stainless steel. However, it is known that oxygen in sodium may result in carbon transport from single-phase monocarbide material. Although care is taken in the experimental procedure to minimize oxygen contamination, significant amounts of oxygen may have been present in some of the capsules, leading to transport of carbon from the fuel; but, neither the monocarbide nor the sesquicarbide phase was attacked to a significant extent under these experimental conditions.

The compatibility of sodium-bonded $UC_{1.43}$ with Type 316 stainless steel and V-15Cr-5Ti alloy capsules is being determined at 750°C in 1000- and 4000-h tests. The as-received ingots were crushed

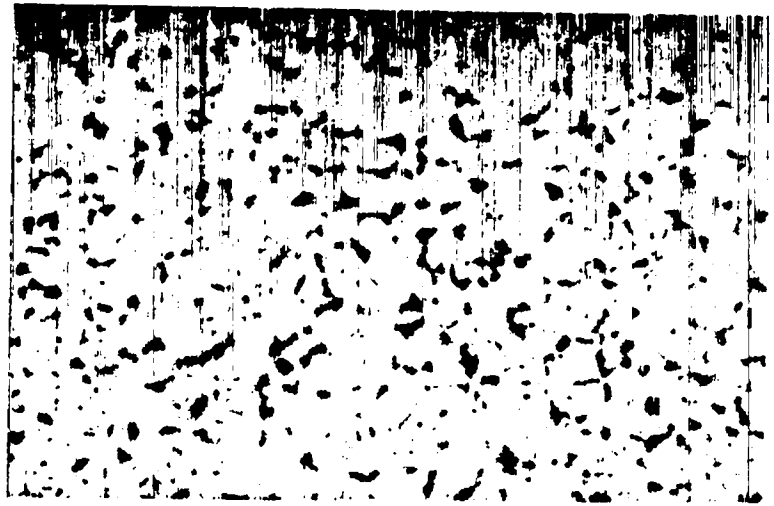

Fig. 464-2. Sigma formation near the bottom closure weld of capsule containing pellets from UNC. Etchant: 20% KOH, 20% $K_3Fe(CN)_6$, H_2O. 300X.

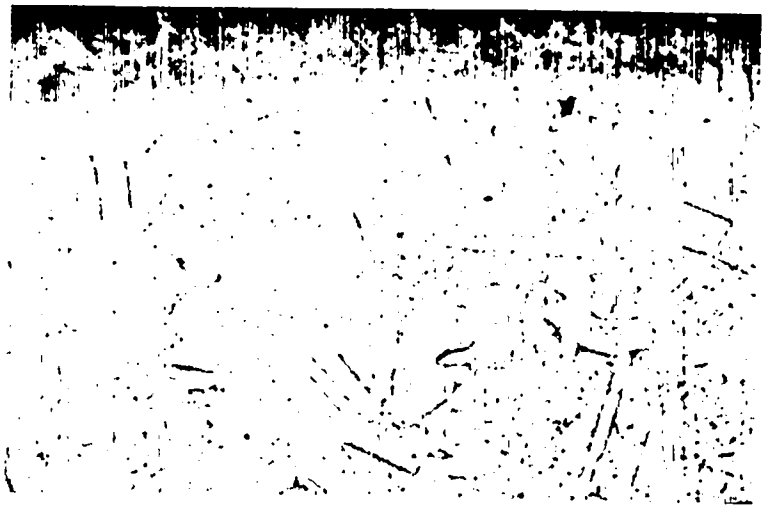

Fig. 464-4. Localized carburized film along the bottom of the capsule that was in contact with UNC pellet. Etchant: 10% oxalic acid, electrolytic. 300X.

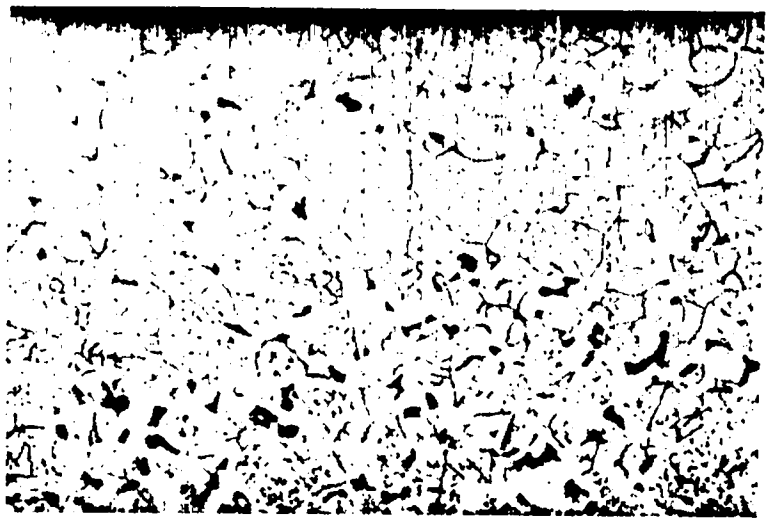

Fig. 464-3. Typical carbide precipitation and sigma formation along the wall of the capsule containing UNC pellets.

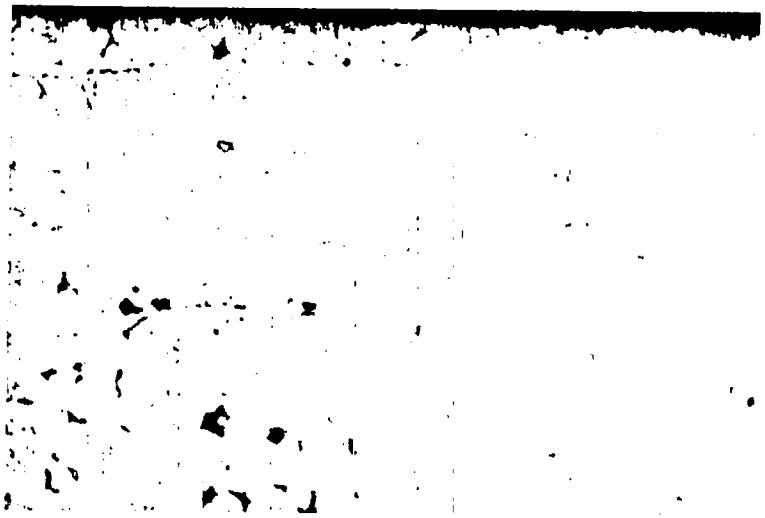

Fig. 464-5. Carburized zone on the wall of a Type 316 stainless steel capsule at junction of two single-phase carbide pellets. Etchant: 10% oxalic acid, electrolytic. 300X.

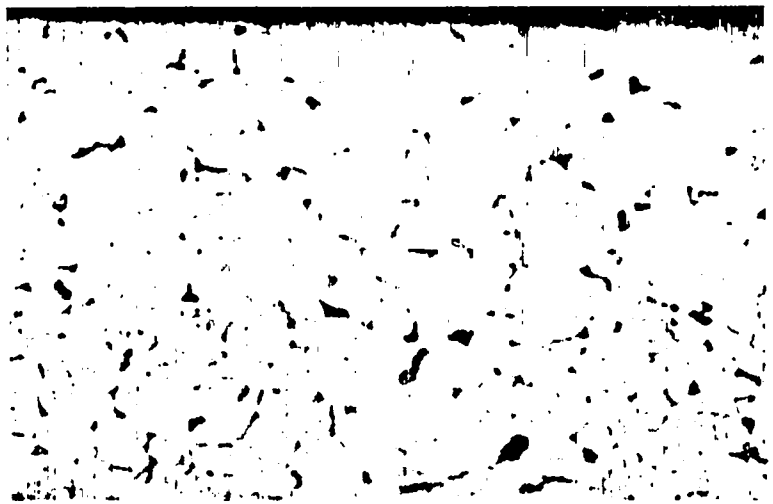

Fig. 464-6. Typical structure of the capsule wall away from the carburized zone shown in Fig. 464-5. Etchant: 10% oxalic acid, electrolytic. 300X.

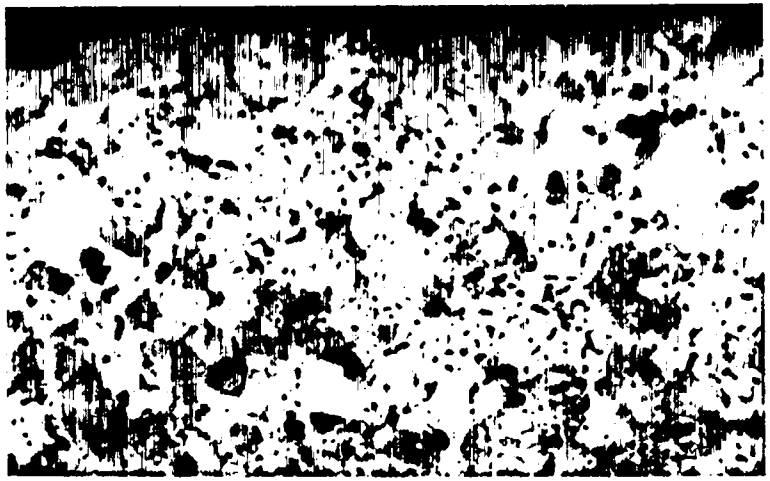

Fig. 464-7. Intergranular attack at the surface of single-phase (U,Pu)C pellet. Etched, 300X.

Fig. 464-8. Attack at the surface of a pellet containing ~ 10 v/o $(U,Pu)_2C_3$ near a region containing acicular phase. Etched, 300X.

Fig. 464-9. Sesquicarbide phase on the surface of a UNC pellet; this phase was unattacked by sodium during the 4000-h compatibility test at 750°C. Etched, 300X.

Table 464-VII

DATA ON THE REACTION OF SODIUM-BONDED $UC_{1.07}$ WITH TYPE 316 STAINLESS STEEL

Capsule No.	Test Time (h)	Temp (°C	Carbon Content (ppm)		Source	
			Type 316L Tab[1]	Sodium[2]	Depth of Decarburization (microns)	Area (cm^2)
1679	500	450	225	100	nil	0.98
1659[3]	500	550	-	-	-	-
1857	500	650	140	50	218	1.36
1854	500	750	90	40	385	1.33
1855[4]	1000	450	-	-	-	1.59
1858	1000	550	240	60	720	1.40
1859	1000	650	350	110	283	1.08
1856	1000	750	570	120	867	1.67

[1]Original carbon content of test tab 175 ppm.
[2]Carbon content of as-received sodium ~ 15 ppm.
[3]Capsule leaked during test.
[4]Test in progress.

to -1/4 in. + 10 mesh under an argon atmosphere and vacuum heat-treated for 100 h at 1350°C. The heat-treated microstructure consisted of a matrix of uranium sesquicarbide containing monocarbide as the second phase. The capsules were loaded and compatibility tests were started during this period.

3. Studies of Carbon Transport in Sodium

The experimental program on the carburization of Type 316L stainless steel in static sodium by an iron-0.87% carbon alloy source was concluded. The rate-controlling step in the carburizing process was the diffusion of carbon in ferrite in the source. A report covering these studies is being written.

4. Solubility of Uranium, Plutonium, and Mixed Carbides in Sodium

A delayed neutron counting procedure is to be used to determine the solubility of ^{235}U, ^{239}Pu, and uranium and plutonium from mixed carbides in sodium as a function of temperature. In these tests, it is planned to heat pellets of the three materials with ~ 100 g sodium for 100 to 1000 h in Ta-10W alloy crucibles. The ^{235}U and the mixed carbide pellets will be tested at 450, 600, and 750°C, while the ^{239}Pu will be tested at only the two lower temperatures. After heating, ~ 2-g samples of sodium will be trepanned in triplicate from the crucible, and the uranium and/or plutonium will be chemically separated and irradiated at ORNL. The test is designed to measure uranium and plutonium solubility in the parts-per-billion range.

Experiments were run with the test apparatus to determine the time required to cool and freeze the sodium after test. These measurements showed that 20.5 min were required to cool the sodium from 750 to 100°C, and that 6.25 min were required to freeze the sodium. Experiments are in progress to improve the apparatus and techniques so the sodium can be chilled at a more rapid rate.

V. SODIUM-BOND HEAT TRANSFER STUDIES
(K. L. Meier)

A. General

The purpose of this project is to evaluate the effects of fuel-pin defects on heat transfer properties of the sodium bond. Such defects could arise in a number of ways. For example, a void in the sodium bond could:

1. Be present before insertion in the reactor.
2. Come from dewetting of the pellet due to change in composition as fission products are formed.
3. Form from a hot spot on the pellet and consequent local vaporization of the sodium, and/or
4. Be produced from desorbed or fission-product gases.

Of these, probably the most serious defect

would be presence of fission gas bubbles in the bond region.

One method of obtaining the high heat fluxes necessary for "defect analysis" consists of utilizing a central, high-heat-flux heater. This method is being utilized at LASL in sodium-bond heat transfer studies.

B. Current Results

Much of the apparatus for out-of-pile testing of sodium bonds utilizing a central, high-heat-flux heater has been fabricated and tested. The completed portions include:

1. Graphite rod heater with boron nitride insulation.
2. UC cylinder.
3. Sodium test loop.

The outer structure of the thermal scanner, which measures the temperature of the "fuel pin" with 40 rotating thermocouples, consists of three subassemblies. Subassemblies 200 (thermocouple rotor) and 300 (inside gas seal and sodium tube) have been fabricated. Construction of subassembly 500 (outer shell and outside gas seal) is 90% complete. The completed parts, including slip rings, motor, mounts, and gears, were assembled. A preset indexer to drive the motor was obtained and connected to the motor. Satisfactory operation was obtained; however, the torque of the motor was barely adequate to drive its assembly. The chief source of friction is the O-rings in the gas seal. Rather than modify the gas seal, it was decided to install a motor with greater torque. The mount was modified to accommodate the new motor.

The mounts which hold the 40 thermocouples were attached to the rotor, and one of the thermocouples was connected to a mount. Operation was satisfactory. The connector plate was attached to the rotor and 80 slip-ring wires were attached. Wiring for the 40 thermocouples was completed from the analog to digital converter through the cable to the connector at the thermal scanner end.

A gas distribution panel was designed and fabrication is 50% complete. This panel distributes nitrogen to the three coolant passages and helium to the heater and thermal scanner. The panel also contains a vacuum circuit to evacuate the thermal scanner. Fabrication of the stand for the thermal scanner was completed, and setup of instrumentation and recorders was begun. Assembly of the heater, cladding, UC cylinder, and the sodium bond has started. This complete assembly will be tested with a heat flux of 10^6 Btu/h-ft^2 prior to use in the thermal scanner.

VI. ANALYTICAL CHEMISTRY
(O. R. Simi, R. T. Phelps)

A. General

Specific analytical techniques have been developed and evaluated to cope with the problems encountered in the investigation of fuel/clad compatibility. The results of many of these special analyses are given in several sections of the report in Project 464. A brief summary of some of the techniques, and the problems to which they were applied, is given below.

B. Current Results

Spectroanalysis of Sodium

An increase in the contaminant concentration levels in the bonding sodium of fuel elements is one important indication of interaction or corrosion. A reliable spectrochemical method, developed previously for measuring contaminants in nonradioactive sodium, was found to be less reliable for analyses of sodium from irradiated fuel elements because of impurities introduced inadvertently during the remote manipulation operations. Further tests of this method were made to determine conditions that would minimize contamination from the hot cell equipment. Before starting the tests, the Solution Processing Cell, which was suspected as the most likely source of contaminants because of corroded metal parts, was carefully cleaned twice, and stainless steel equipment that contacted samples directly was replaced by tantalum or lucite pieces. Readily available pure NaCl, rather than less pure elemental sodium, served as the test material. The samples were dissolved in DOWANOL EB and HCl, and the solutions evaporated to dryness in a closed system with provision for absorption of acid fumes. In the Weighing Cell and the Spectrochemical Analysis Cell, the NaCl residue was mixed with an equal weight of graphite containing 100 ppm of germanium for an internal standard, and a 10-mg electrode portion was arced. Spectra for samples and standards were recorded on S.A.-3 photographic plates by use of a 3.4-meter Ebert-mounting spectrograph, and results were evaluated by visual comparison or

by photometry.

Analyses of five separate samples of NaCl showed that Al, Cr, Cu, Fe, and Si impurities were still observed but at much lower concentration than in the initial tests. The impurities appeared randomly in perhaps one out of four spectra. A series of tests made out-of-cell indicated that the major source was spot impurities in the electrodes which were enhanced by the NaCl. Steps planned to reduce the effect of spot impurities include increasing the sample size and electrode crater depth, preburning the electrodes, and using a denser grade of graphite.

VII. PUBLICATIONS

F. B. Litton and A. E. Morris, "Carburization of Type 316L Stainless Steel in Static Sodium," submitted for publication in J. Nucl. Mater.

PROJECT 465

REACTOR PHYSICS

Person in Charge: D. B. Hall
Principal Investigator: G. H. Best

I. INTRODUCTION

Basic to the evaluation of various fast breeder concepts and proposals are the analytical techniques and physical data used in the analyses. Valid comparisons between different concepts and proposals depend on minimization of differences in results due to methods of analyses. To this end, the Los Alamos Scientific Laboratory is cooperating with other AEC laboratories and contractors in the development of evaluated cross-section data and associated processing codes. In addition, the Laboratory is working on the development and maintenance of digital computer programs pertinent to the nuclear analysis of fast breeder concepts. The Laboratory is also adapting, modifying, and evaluating modular programming systems for comprehensive nuclear analysis. Finally, the Laboratory is evaluating the performance characteristics of various fast breeder reactor concepts.

II. CROSS-SECTION PROCUREMENT, EVALUATION, AND TESTING (M. E. Battat, D. J. Dudziak, R. J. LaBauve, R. E. Seamon)

A. General

Accurate predictions of reactor design parameters, such as critical mass, material worths, and spectral response, require the development and maintenance of up-to-date basic microscopic nuclear data files. To meet this end, a national cooperative program is in progress to prepare an evaluated nuclear data file (ENDF/B). The large amount of experimental data which is becoming available, together with theoretical data, makes the maintenance of ENDF/B a continuing task. In addition, a large effort is needed in evaluating and testing the microscopic data prior to use in reactor calculations.

B. Data Testing

At its September 1969 meeting, the Codes and Formats Subcommittee of the Cross Section Evaluation Working Group (CSEWG) tentatively adopted a new format for storage of photon production data. The acceptance of the new format was contingent upon the submission of a detailed format and procedures document to supersede LA-3801, as well as on commitments by other laboratories to revise the CHECKER and PLOTFB codes. The Los Alamos Scientific Laboratory undertook the task of retranslating photon production data for sodium, magnesium, chlorine, potassium, and calcium into the new format, as well as rewriting of the LAPH and PHOX codes.

A new version of LA-3801 has been drafted to define the new format and procedures in detail. The new format is logically equivalent to the old but is restructured into new file numbers; it had not yet been carefully documented at the time of the Codes and Formats Subcommittee meeting. The revision of LA-3801 contains the equivalent of a Procedures Manual, with a section for procedures being included in each ENDF/B photon production data file, as well as in each photon interaction data file. The draft is presently being reviewed within LASL. The document will next be sent to contributors at other laboratories for review prior to issuance as a format report. The sodium data[1] presently in the ENDF/B Data File in the original photon production data format has been translated to the revised format. These translated data will be included in an appendix of the report as a sample case.

All of the photon production cross-section data that have been translated into the original ENDF/B format (viz., sodium, magnesium, chlorine, potassium, and calcium) have been received from the University of Virginia (UVa) and checked for completeness. Also, listings of PHOX runs[1] on the data are being reviewed. These "physics" checks on the photon data will be used to correct the data files, where necessary, although a preliminary examination shows no serious errors. All of the data have been checked for format syntax errors with the CHECKER code.

The final draft of a UVa report describing the data review and a "physics" testing code for ENDF/B photon production data has been reviewed and submitted to the Defense Atomic Support Agency (DASA), the funding agency, for publication approval.

C. Processing Codes

1. FLANGEII and GLEN. Work on a code to generate multigroup-multitable (MULTAB) cross sections from ENDF/B thermal data is continuing. The GLEN code has been linked to the FLANGEII code, and ENDF/B thermal data for H_2 bound in H_2O is being used for checking of results. The FLANGEII code is used for generating fine-group cross sections, including an inelastic scattering kernel for the ENDF/B material being processed. GLEN is used for generating an infinite-medium spectrum used in collapsing to broad-group cross sections, which the code outputs in the DTF-IV format.

FLANGEII also makes a very accurate calculation of the total inelastic cross sections directly from the $S(\alpha,\beta)$ data on the ENDF/B tape. As an option in the code, these total cross sections can be used to normalize the scattering kernels output by the code.

In GLEN, the total cross sections are obtained by integration of the scattering kernels provided by FLANGEII. As a check, these are compared with the results from FLANGEII in Figs. 465-1 and 465-2 for the P_0 and P_1 scattering components, respectively. These figures indicate the following:

a. Unnormalized kernels cannot be used in GLEN. (This is unfortunate in that considerable machine time is required for the FLANGEII integrations.)

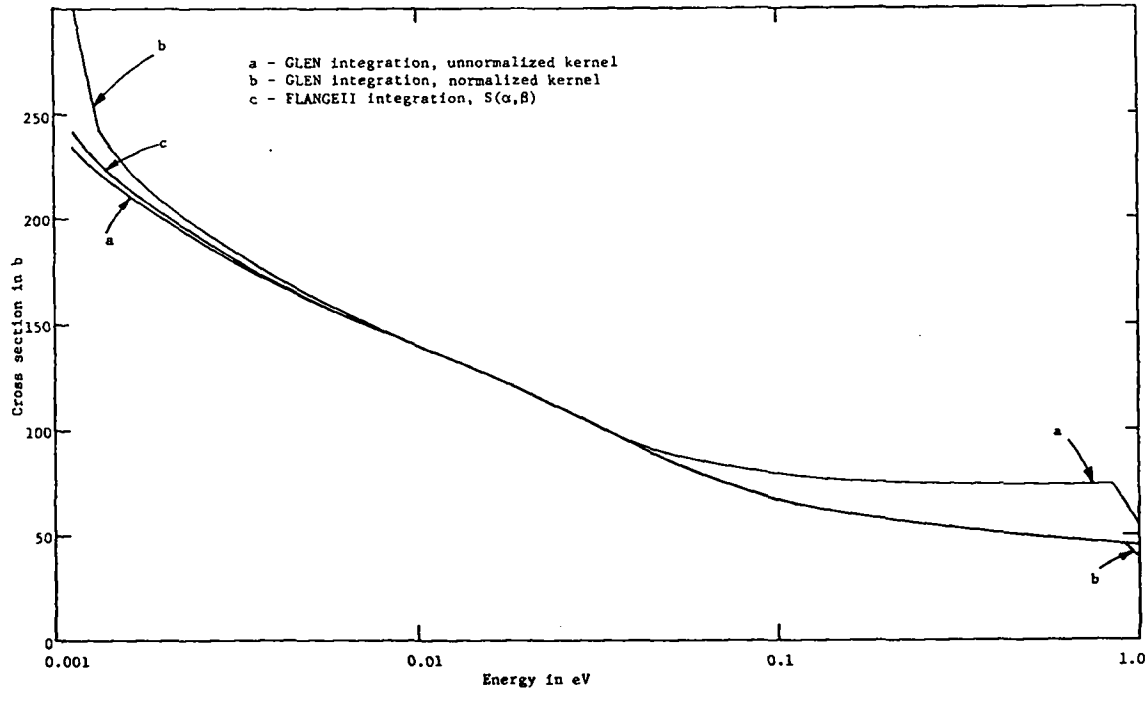

Fig. 465-1. H_2O total inelastic cross section, P_0 component.

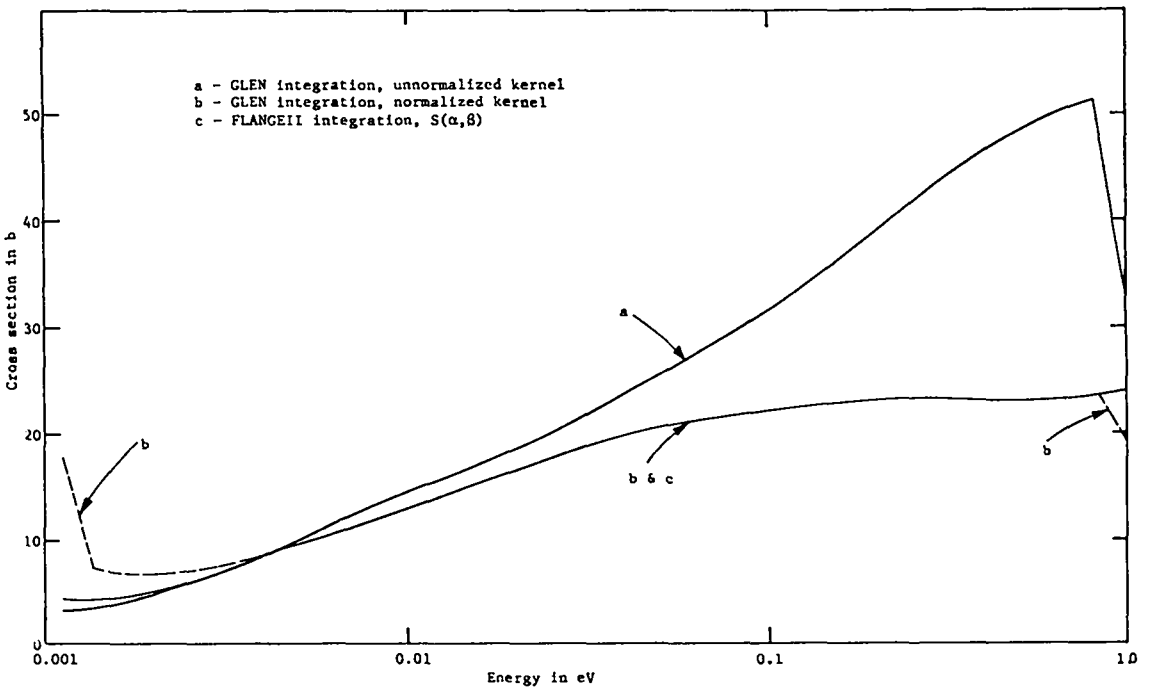

Fig. 465-2. H_2O total inelastic cross section, P_1 component.

b. End-point integrations in GLEN seem to be inaccurate.

c. Low-energy values for the scattering kernels seem to be in error.

It is felt that a finer-energy mesh could be used to improve b and c.

Further tests of these cross sections will be made by using them in the DTF-IV code to calculate a H_2O-^{235}U (300:1) system.

2. PHOX. A preliminary review of the PHOX code has been made to estimate the effort required to revise it, in order to accept the revised photon production data format.

3. Utility Codes. LASSO and other utility codes written for translating data to the revised format have been placed on an UPDATE tape for the CDC-6600 computer. The utility codes do simple tasks, such as sequence number checking and resequencing.

The CHECKER, LUTE, LATEX, FIXLUTE, and FIXUKTP codes have been received on tape from UVa and have been placed on an UPDATE tape. The CHECKER code was compiled from the UPDATE tape and debugged on the CDC 6600. It has been used to check the format syntax of the sodium data. This version of CHECKER had been extended at Brookhaven National Laboratory (BNL) and Oak Ridge National Laboratory (ORNL) to check the photon production data and was further modified at UVa to accept MT = 110. Both LUTE and LATEX have now been documented in UVa Report No. NE-3383-102-694, which will be distributed by BNL to the ENDF/B distribution list under the document number ENDF-128. FIXLUTE is a code written at UVa to check normalization of photon secondary angular and energy distributions, renormalize to unity, and produce a corrected ENDF/B tape. FIXUKTP is a code, also written at UVa, to correct data which is in the United Kingdom Atomic Energy Authority (UKAEA) format. It is analogous to the ENDF/B code CRECT.

D. Shielding Methods

Revisions have been made in the LAPH code to incorporate DTF-IV input routines and new subroutines that combine the photon production matrices in each zone with the appropriate densities, as specified by the zone composition in DTF-IV format. Photon production and photon energy production matrices

and source vectors are now calculated within the same pass through the code. The numerical integrations over the neutron fine groups are performed with the trapezoidal rule, using the same energy mesh as that used in specifying the cross-section data in File 3 of the ENDF/B tape. The subroutine that reconstructs the photon cascades from transition probability arrays has been rewritten to save core and to eliminate the calculation of those quantities that are energy independent at each energy of the neutron integration mesh. The code checks that the values of $\bar{E}_g$, the effective average energy for each gamma group, are such that $E_g \leq \bar{E}_g \leq E_{g+1}$, where E_g and E_{g+1} are the boudaries of a particular gamma group. If this condition is not met, an input error warning is printed, and the incorrect value is replaced by the value of the energy at the midpoint of the interval. The code has been restructured in an overlay arrangement to incorporate these changes. In OVERLAY (1,0), the input is read in DTF-IV format, and a binary tape for use as input to OVERLAY (2,0) is prepared; in OVERLAY (2,0), the photon production and photon energy production matrices for each material in each zone are calculated; in OVERLAY (3,0), the matrices are combined, and the photon source and energy source vectors are calculated for each mesh interval. The output options are being modified to agree with those specified in a recent revision of the LAPH Input Instructions. An LA report[2] documenting the code will be published within the next two months, and an abstract of the code has been submitted to Nuclear Science and Engineering. A problem similar to the sample problem to be used for the code documentation has been run; it required about 5.6 min of central processor time, 8.4 min of peripheral processor time, and about $140{,}000_8$ core locations.

III. REACTOR ANALYSIS METHODS AND CONCEPT EVALUATION

A. General

A continuing task in fast reactor analysis and evaluation is the improvement of computer programs and the development of new computational methods. In addition to new methods, advances are constantly being made in computer technology which make possible the extension of existing calculational techniques.

B. Preparation and Maintenance of Code Packages

1. Computer Code Coordination (B. M. Carmichael, T. J. Hirons, G. C. Hopkins). The DAC1 code[3] and a two-dimensional version of the same code, DAC2, are included in the set of codes adopted by the *de facto* Committee on Computer Code Coordination. This committee consists of representatives from several laboratories selected by the AEC to study the problems of adapting reactor codes to various types of computers and the problems of interfacing reactor codes from different organizations in linked calculations. A tentative schedule covering the current and next fiscal years has been prepared for adapting DAC1 and DAC2 to the standard specifications to be formulated by the committee.

2. Modular Programming Systems (F. McGirt). The modification of the Knolls Atomic Power Laboratory (KAPL) DATATRAN System[4] for use at LASL is nearly complete. This has resulted in a modular programming system[5] (LAMPS) that provides the basic features of DATATRAN on our machines.

Since most of the work with LAMPS has been directed toward making the system operational at LASL, only a few of the many features of LAMPS have been employed. Free-standing codes have been linked using LAMPS with very little modification of these codes.[6] Geometry-processing modules from the KAPL iterative transport package have been compiled and added to the system. Modules that generate cross-section sets from ENDF/B data tapes are being obtained from KAPL.

A reduced field length version of LAMPS is available to users of the LASL remote terminal systems. Due to a shortage of permanent disk files, a magnetic tape containing absolute overlays of the system programs must be assigned for each LAMPS job.

The feasibility of using components of the Argonne modular system[7] (ARC) on LASL computers is being investigated. Instead of trying to load the complete modular system as with DATATRAN, the one-dimensional transport theory standard path PTR1D is being used. One of two possible approaches in loading PTR1D will be tried. The first possibility is to use the PTR1D standard path as a structured overlay system. The second is to use only the computational module NUC003 of PTR1D and supply the input and output requirements, using LAMPS data

lists. A choice of method will be made after consultation with Argonne and after more extensive examination of the ARC system.

Free-standing codes, written in FORTRAN IV either at LASL or other installations, may now be run, using LAMPS data lists to handle input and output. In addition, most DATATRAN modules can be used directly in the system. These provide the basis for a powerful computational capability for reactor developmental work. If it proves possible to include ARC modules without extensive reprogramming, the computational capability can be easily further enhanced.

3. Burnup Code (T. J. Hirons). The burnup-refueling code,[8] PHENIX, is being modified to allow the option of performing an entire fuel-cycle analysis in one run. This complete analysis begins with the clean reactor and proceeds through the approach to equilibrium. The number of burnup intervals required to reach equilibrium is a direct function of the particular fractional-batch refueling scheme.

An abstract of PHENIX has been accepted for publication in Nuclear Science and Engineering.

4. Diffusion Code Development (J. C. Vigil). Programming, compiling, and testing of the 3-Dimensional Diffusion Theory code (3DDT) have been completed. This code is an extension to three space dimensions of the 2DB code.[9] All of the 2DB features were retained in 3DDT, except that the geometry options are X-Y-Z and R-θ-Z. Briefly, some of the features are:

- Multigroup calculations of k_{eff} or criticality searches on reactor composition, reactor dimensions, or time absorption (α) by means of either the regular or the adjoint flux equations,
- Computation of material burnup,
- Restriction to downscattering,
- Variable dimensioning for maximum use of available fast memory,
- Group rebalancing and successive overrelaxation with line inversion,
- Searches on compositions or dimensions with values of α or k_{eff} as parametric eigenvalues (i.e., user selected), and
- DTF-IV input format.[10]

Both Extended Core Storage (ECS) and disk storage are utilized in 3DDT. In general, four-dimensional arrays [e.g., $\phi(x,y,z,E)$] are stored on disk; three-dimensional arrays [e.g., $\phi(x,y,z)$ for a particular energy group] are stored in ECS; and two-dimensional arrays [e.g., $\phi(x,y)$ for a particular group and axial mesh point] are stored in the fast central memory. Thus, central memory storage requirements are insensitive to the number of energy groups and the number of axial mesh points.

The variable dimensioned arrays in central memory require N_{cm} core storage locations where

$$N_{cm} = 17\times IM\times JM + ITL\times MT + 15\times ML + 2\times JM\times KM + 4\times M01 + 3\times IGM + 4\times IZM + 2\times(IP+JP+KP) + 2\times(IM+JM+KM) + 4\times ML\times IZM + 2\times MAX(IM,JM) + T06\times(IM+JM+KM+IZ+JZ+KZ) . \quad (1)$$

ECS (N_{ecs}) and disk (N_{dk}) storage requirements are

$$N_{ecs} = 10\times IM\times JM\times KM + IM\times JM\times M06 + IGM\times(JM\times KM+IM\times KM+IM\times JM) \quad (2)$$

$$N_{dk} = 6\times IM\times JM\times KM\times IGM + ITL\times MT\times IGM . \quad (3)$$

In Eqs. 1 through 3,

IM = number of radial (or X) mesh points,
JM = number of rotational (or Y) mesh points,
KM = number of axial (Z) mesh points,
ITL = cross section table length,
MT = total number of materials including mixes,
ML = number of material cross sections read from cards,
M01 = number of mixture specifications,
IGM = number of energy groups,
IP = IM + 1,
JP = JM + 1,
KP = KM + 1,
IZM = number of material zones,
IZ = number of radial (X) zones to be modified (delta option),
JZ = number of rotational (Y) zones to be modified (delta option),
M06 = number of R-θ (or X-Y) planes with unique zone numbers, and
T06 = 1 for delta calculations, = 0 otherwise.

For a fairly large problem in which IM=JM=KM=M06=IZ=JZ=KZ=30, IGM=16, ITL=12, MT=100, ML=20, M01=200, IZM=80, and T06=1, the storage requirements for the variable arrays are:

N_{cm} = 28,574

N_{ecs} = 340,200

N_{dk} = 2,611,200.

These requirements are well within the capacities of our CDC-6600 computing equipment.

Calculations with 3DDT in R-θ-Z and X-Y-Z geometries were compared with corresponding two-dimensional calculations with the 2DB code. The results of various test problems are described below.

a. Two-Group, R-θ-Z Test Problems. The first series of 3DDT calculations consisted of two-group k_{eff} (both regular and adjoint), alpha, concentration, and delta computations of a two-region cylindrical reactor in R-θ-Z geometry. For these test problems, material compositions were constant in the θ direction, and, thus, the reactor could be represented exactly in an R-Z calculation. The core region was a solid vertical cylinder with radius = 85.88 cm and height = 99.06 cm. A reflector medium surrounded the core axially (27.4-cm-thick top and bottom) and radially (20.8-cm thick). Compositions of the core and reflector regions are given in Table 465-I.

TABLE 465-I

COMPOSITIONS OF CORE AND REFLECTOR REGIONS

R-θ-Z Test Problems

Nuclide	Atom Density, Units of 10^{24}/cm^3	
	Core	Reflector
Al	1.22×10^{-4}	1.34×10^{-4}
B	0.92×10^{-7}	1.29×10^{-7}
C	7.87×10^{-2}	7.97×10^{-2}
Fe	3.91×10^{-5}	4.50×10^{-5}
^{234}U	7.05×10^{-8}	
^{235}U	7.41×10^{-6}	
^{238}U	4.58×10^{-7}	

Because of symmetry, only the upper half of the reactor was represented in both the 2DB and 3DDT calculations, and a reflective boundary condition was applied to the bottom boundary. In addition, only a 15° sector of the θ dimension was represented in the R-θ-Z calculation. Periodic and reflective boundary conditions on the θ boundaries are equivalent in this configuration and, thus, should give the same results. This was indeed found to be the case.

All common input data (mesh intervals, cross sections, convergence parameters, initial flux guess, etc.) for the R-Z and R-θ-Z calculations were identical. The meshes contained 21 intervals radially, 15 axially, and 5 in the θ direction. Thus, the R-θ-Z problem contained five times more mesh points than the R-Z problem. Initial flux guesses were computed internally in the codes from cosine distributions in the radial and axial directions and a flat distribution in the θ direction. Convergence criteria typical of actual production runs were used in all the calculations. These criteria were: lambda or total fission source convergence criterion = 0.0001, pointwise flux convergence criterion = 0.001, and eigenvalue search convergence criterion = 0.001.

The first calculation for the two-group R-θ-Z test configuration was a regular k_{eff} computation, followed automatically by a burnup interval of 30 days at 3 MWT total power and a computation of the k_{eff} for the depleted inventory. Results of the two- and three-dimensional calculations are shown in Table 465-II. In absolute magnitude, the

TABLE 465-II

REGULAR k_{eff} CALCULATIONS
WITH 30-DAY BURNUP AT 3 MWT

Two-Group, R-θ-Z Problem

	2DB	3DDT	3DDT/2DB
Initial k_{eff}	1.0557	1.0553	0.9996
Final k_{eff}	1.0502	1.0499	0.9997
Reactivity change (Δk/k)	-0.0052	-0.0051	0.98
^{235}U depletion (g)	112.8	112.8	1.000
Breeding ratio	0.0045	0.0045	1.000
Computation time (sec)	15.3	83.2	5.4

initial and final k_{eff}'s both agreed within 0.0004, and the reactivity changes due to burnup agreed within 0.0001. The amounts of ^{235}U depleted were in complete agreement, as were the breeding ratios (the core contained small amounts of ^{234}U and ^{238}U). Both before and after depletion, group fluxes from 2DB and 3DDT were in agreement within 0.2% at all mesh points. (At most mesh points, the disagreement was only 0.1%.) The computing time, defined as central processor (CP) time exclusive of compilation time, was 5.4 times longer for the 3DDT calculation than for the 2DB calculation.

The 3DDT calculation of Table 465-II was performed with reflective boundary conditions at the θ boundaries. With periodic boundary conditions, exactly the same results were obtained, except that the computing time was 95 sec instead of 83 sec. This result was expected, since the algorithm for performing line inversion* is more complicated for periodic than for reflective boundary conditions.

The next calculation for the two-group R-θ-Z configuration was an adjoint k_{eff} calculation. Results, which are shown in Table 465-III, were similar to those obtained for the regular problem

TABLE 465-III

TWO-GROUP, R-θ-Z CALCULATIONS

	2DB	3DDT	3DDT/2DB
Adjoint k_{eff}			
k_{eff}	1.0557	1.0553	0.9996
Computing time (sec)	13.9	78.3	5.6
Alpha Search			
Alpha (sec^{-1})	116.3	115.7	0.995
Prompt neutron generation time (sec)	4.79×10^{-4}	4.78×10^{-4}	0.998
Computing time (sec)	17.6	113	6.4
Concentration Search			
Eigenvalue	0.8461	0.8475	1.002
Computing time (sec)	16.8	98.7	5.9

(Table 465-II). For both 3DDT and 2DB, the k_{eff} computed in the adjoint problem agreed with the k_{eff} computed in the regular problem. Note that the computing time for 3DDT was 5.6 times longer than that for 2DB. Adjoint group fluxes from 3DDT and 2DB typically agreed within 0.1%, and the maximum disagreement was 0.3%.

Eigenvalue searches on time absorption (alpha), critical uranium composition (concentration), and critical core dimensions (delta) were also performed for the two-group R-θ-Z configuration. Results of the alpha calculations are also shown in Table 465-III, where it is seen that the 2DB and 3DDT values for alpha agreed within 0.5%. Since $\alpha = (k_{eff} - 1)/\ell$, where ℓ is the prompt neutron generation time, the disagreement in α is consistent with the disagreement in k_{eff}. That is, the ratio $\alpha(3DDT/\alpha(2DB)$ differs by only 0.2% from the ratio $[k_{eff}(3DDT) - 1]/[k_{eff}(2DB) - 1]$.

*Simultaneous solution of fluxes for mesh points lying on the same line by Gaussian elimination and back-substitution.

Since k_{eff} and α were obtained from separate calculations, the prompt neutron generation time could be derived from $\ell = (k_{eff} - 1)/\alpha$. As seen in Table 465-III, values of ℓ derived from 2DB and 3DDT calculations agree within 0.2%. For the alpha calculation, the computing time with 3DDT was 6.4 times longer than with 2DB, and group fluxes typically agreed within 0.1%. (Maximum disagreement was 0.2%.)

Results of the concentration search calculations are shown in Table 465-III. The eigenvalue in this case is the factor by which all the uranium atom densities in the core must be multiplied to yield a critical system. As seen in Table 465-III, 2DB and 3DDT disagree by 0.2% and the disagreement is in a direction consistent with the disagreement in k_{eff}. The computing time with 3DDT was 5.9 times longer than with 2DB. Group fluxes typically agreed within 0.1%, and the maximum disagreement was 0.4%.

Results of the delta calculations are summarized in Table 465-IV. Three separate calculations were made. In the first, the core height was held

TABLE 465-IV

CRITICAL DIMENSIONS SEARCH CALCULATIONS

Two-Group, R-θ-Z Problem

	2DB	3DDT	3DDT/2DB
Search on:			
Core radius (core height held constant at 99.06 cm)			
Eigenvalue	- 0.1137	- 0.1139	1.002
Critical radius (cm)	76.12	76.10	0.9997
Computing time (sec)	17.8	110	6.2
Core height (core radius held constant at 85.88 cm)			
Eigenvalue	- 0.1519	- 0.1508	0.993
Critical height (cm)	84.02	84.12	1.001
Computing time (sec)	17.2	138	8.0
Both height and radius			
Eigenvalue	- 0.0703	- 0.0707	1.006
Critical height (cm)	92.10	92.06	0.9996
Critical radius (cm)	79.85	79.81	0.9995
Computing time (sec)	18.1	118	6.5

constant, and a search was made on the core radius. In the second, the core radius was held constant, and the core height was varied to achieve a critical system. Finally, both the core radius and height were varied by the same factor to achieve criticality in the third calculation. In the delta calculations, the adjusted dimension, say L, is

given in terms of the initial dimension, L_0, by $L = L_0(1 - EV)$ where EV is the eigenvalue given in Table 465-IV. Critical core dimensions computed with the 2DB and 3DDT codes agree within 0.1% or better. Group fluxes typically agreed within 0.2% with a maximum disagreement of 0.4%. Computing times with 3DDT ranged from 6.2 to 8.0 times longer than with 2DB.

b. X-Y-Z Test Problems. The second series of 3DDT calculations consisted of two- and three-group regular k_{eff} computations of a two-region parallelepiped in X-Y-Z geometry. For these calculations, material compositions were homogeneous in the Z direction. Furthermore, the top and bottom boundaries in the X-Y-Z calculation were reflected to simulate an infinite height. Thus, the configuration could be represented exactly in an X-Y calculation with 2DB. In the X-Y plane, the reactor consisted of a square (150 x 150 cm) core region, surrounded by 25 cm of reflector on all four sides. A height of 20 cm was used in the X-Y-Z problem. Compositions of the core and reflector regions were the same as those in Table 465-I, except that the uranium atom densities were reduced to 0.4 of those in Table 465-I.

Because of symmetry, only one quadrant of the X-Y cross section was represented in the calculations, and reflective boundary conditions were applied to the left and front boundaries. As in the previous calculations, all common input data for the X-Y and X-Y-Z calculations were identical. The meshes contained 21 intervals in the X direction, 20 in the Y direction, and 5 in the Z direction. Thus, the X-Y-Z problem contained five times more mesh points than the X-Y problem. Convergence criteria were the same as those specified for the R-θ-Z problems.

Results of the X-Y-Z calculations are summarized in Table 465-V. For the two-group calculations, the k_{eff}'s computed with 3DDT and 2DB agreed within 0.09%, group fluxes typically were in agreement within 0.3% with a maximum disagreement of 0.6%, and the computing time was 6.1 times longer with 3DDT. Since a two-group calculation does not test completely that portion of the code that computes downscatter sources, a three-group computation was performed. For this case, the k_{eff}'s computed with 3DDT and 2DB agreed within 0.12%, group fluxes typically agreed within 0.4% (maximum disagreement was 1%), and the 3DDT computing time was 7.1 times longer.

TABLE 465-V

REGULAR k_{eff} CALCULATIONS

X-Y-Z Problem

	2DB	3DDT	3DDT/2DB
Two-Energy Groups			
k_{eff}	1.0084	1.0075	0.9991
Computing time (sec)	15.1	91.4	6.1
Three-Energy Groups			
k_{eff}	1.0138	1.0126	0.9988
Computing time (sec)	17.5	124	7.1

Results of all the test calculations indicate that the 3DDT code is performing satisfactorily. In general, the ratio of 3DDT to 2DB computing time was approximately the same as the mesh point ratio. Extrapolating from the test problems, it is estimated that a six-group 3DDT problem, containing 30 x 30 x 30 mesh points, would require about 60 min of computing time on the CDC-6600 computer. This time is about the same as that required for a six-group S_4 problem containing 30 x 30 mesh points. On the CDC-7600 computer, which is purported to be four times faster than the CDC-6600, even larger problems should be practicable.

Future work on 3DDT is contemplated in the following areas (not necessarily listed in order of priority):

1. Incorporation of internal boundary conditions (principally for control-rod problems),
2. Incorporation of a spherical (R-θ-φ) geometry option (present version has X-Y-Z and R-θ-Z options),
3. Incorporation of a subroutine to compute neutron balance by zone (present version computes only the overall neutron balance),
4. Incorporation of a subroutine to compute neutron currents for use in a three-dimensional perturbation code,
5. Incorporation of a subroutine to compute activities by zone and material,
6. Incorporation of a subroutine to compute poisoning by xenon and samarium, and
7. Extension of the code to allow upscattering (present version is restricted to downscattering).

C. Fast Reactor Design Analysis

1. Fuel-Cycle Analysis (T. J. Hirons). A complete fuel-cycle analysis has been performed on a recent advanced LMFBR design.[11] This reactor has a core H/D of 0.44, an increase of a factor of 2.5 over the pancake design[12] analyzed previously. The two-dimensional diffusion-burnup-refueling code[8] PHENIX was used for the analysis. Several reactor characteristics at the midpoint of the equilibrium cycle were tabulated and compared with those given in the design report. Values for the core fissile loading, breeding ratio, and core conversion ratio agreed very closely with the design values, while the burnups were 15 to 20% higher than the specified 112,200 MWd/Te.

The mass balances from the above-mentioned analysis were processed through LAFF and the Los Alamos Reactor Economics Code (LAREC). LAFF takes the charges and discharges from the fuel-cycle analysis, along with the appropriate load history, and prepares a set of mass balances for input to LAREC. LAREC then performs the complete economic analysis for the given reactor system and calculates a power cost in mills/kWh.

Additional parametric studies will be performed on this reactor; quantities to be varied include the length of the burnup time step, the load history, and the capital costs.

2. Space-Energy Collapsing Scheme Applicable to Fast Reactor Fuel-Cycle Analysis (R. E. Alcouffe, T. J. Hirons). The space-energy collapsing scheme applicable to fast reactor fuel-cycle analysis described in the previous quarterly report[13] is being prepared as an article for Nuclear Science and Engineering. The fuel-cycle analysis discussed in the previous section was performed using eight-group cross sections obtained from a 49-group fundamental-mode collapsing spectrum, i.e., ENDF/B data processed directly from MC^2 into broad-group constants. In this fuel-cycle analysis, separate cross-section sets for the core and blanket regions were used. To compare the effects of two-dimensional versus fundamental-mode collapsing spectra on this advanced system, a 49-fine-group reference calculation was performed using ENDF/B cross-section data processed by MC^2 but with no broad-group collapsing. For the clean reactor, errors in the eight-group calculation for k_{eff} and breeding ratio were +0.6 and -1.5%, respectively. These errors are slightly less than those obtained from the analysis of the pancake mixed-oxide design,[12] which has an overall softer spectrum. The 49-group two-dimensional spectrum will be used to collapse the cross sections and leakage coefficients to eight- and four-broad-group structures; complete fuel-cycle analyses will then be performed using these structures.

D. Computational Techniques for Repetitively Pulsed Reactors (G. C. Hopkins)

Work has been completed on the calculational methods for repetitively pulsed reactor systems. Both linear and nonlinear forms of reactivity were included in the study that will be detailed in an LA report.

IV. CURRENT PUBLICATIONS

1. Thomas J. Hirons and R. Douglas O'Dell, "Calculational Models for Fast Reactor Fuel-Cycle Analysis," submitted to Nuclear Applications.

2. Morris E. Battat, Robert J. Seamon, and Raphael J. LaBauve, "Comparison of Several Versions of the MC^2 Code," presented at "Multigroup Cross Section Preparations Seminar, Oak Ridge, Tennessee, October 1 and 2, 1969. Published in Proceedings.

3. R. Douglas O'Dell and Thomas J. Hirons, "PHENIX, Burnup-Refueling Code," submitted to Nuclear Science and Engineering.

4. Thomas J. Hirons, R. Douglas O'Dell, and Raymond E. Alcouffe, "Spectral Effects on Calculated Fuel-Cycle Parameters in Large Fast Breeders," presented at ANS 1969 Winter Meeting, November 30 to December 4, 1969, San Francisco, California. Published in Proceedings.

5. George C. Hopkins, "Calculational Methods for Repetitively Pulsed Reactors," presented at ANS 1969 Winter Meeting, November 30 to December 4, 1969, San Francisco, California. Published in Proceedings.

6. Barry K. Barnes, W. Mort Sanders, and Dale M. Holm, "Analysis of Fuel-Element Sections by Two-Dimensional Gamma Scanning," presented at ANS 1969 Winter Meeting, November 30 to December 4, 1969, San Francisco, California. Published in Proceedings.

REFERENCES

1. Donald J. Dudziak, "Translation to ENDF/B and 'Physics' Checking of Cross Sections for Shielding," NE-3383-104-694 (or ENDF-130), University of Virginia (1969).

2. Donald J. Dudziak, Alan H. Marshall, and Robert E. Seamon, "LAPH, A Multigroup Photon Production Matrix and Source Vector Code for ENDF/B," LA-4337, Los Alamos Scientific Laboratory (in press).

3. B. M. Carmichael, "DAC1, A One-Dimensional S_n Perturbation Code," LA-4342, Los Alamos Scientific Laboratory (in press).

4. H. J. Kopp, J. D. Morris, and W. E. Schilling, "DATATRAN Modular Programming System for Digital Computers," KAPL-M-6997, Knolls Atomic Power Laboratory (1968).

5. Private communication.

6. Private communication.

7. B. J. Toppel, "The Argonne Reactor Computation (ARC) System," ANL-7322, Argonne National Laboratory (1967).

8. R. Douglas O'Dell and Thomas J. Hirons, "PHENIX, A Two-dimensional Diffusion-Burnup-Refueling Code," LA-4231, Los Alamos Scientific Laboratory (in press).

9. W. W. Little, Jr. and R. W. Hardie, "2DB User's Manual," BNWL-831, Battelle Northwest Laboratory (1968).

10. K. D. Lathrop, "DTF-IV, A FORTRAN-IV Program for Solving the Multigroup Transport Equation with Anisotropic Scattering," LA-3373, Los Alamos Scientific Laboratory (1965).

11. "Comparison of Two Sodium-Cooled 1000 MWe Fast Reactor Concepts; Task 1, Report of 1000 MWe LMFBR Follow-On Work," GEAP-3618, General Electric (1968).

12. "Liquid Metal Fast Breeder Reactor Design Study (1000 MWe UO_2-PuO_2 Fueled Plant)," GEAP-4418, General Electric (1963).

13. "Quarterly Status Report on the Advanced Plutonium Fuels Program, July 1 to September 30, 1969," LA-4307-MS, Los Alamos Scientific Laboratory (1969).

PROJECT 467

FUEL IRRADIATION EXPERIMENTS

Person in Charge: D. B. Hall
Principal Investigators: R. H. Perkins
J. C. Clifford

I. INTRODUCTION

The goal of this program is to examine the irradiation behavior of advanced fuels for LMFBRs. At present, the fuel concepts under study are sodium-bonded mixed carbides and metals. However, because of the decreasing interest in metals as LMFBR fuels, metal fuel work has been reduced and will be terminated by the end of the fiscal year.

Carbide investigations center around the irradiation performance of high purity, single-phase $(U_{0.8}Pu_{0.2})C$ produced and characterized at the Los Alamos Scientific Laboratory (Project 463). Sodium-bonded, mixed-carbide pins are being irradiated in the EBR-II reactor at heat ratings of interest for fast reactor application. The experiments are designed to examine the degree of fuel swelling, gas release, fuel-sodium-clad interaction, and the migration of fissionable material and fission products as a function of burnup and fuel density. Thermal flux irradiations of LASL-produced carbides also are included to augment determination of the effects of high burnup on fuel-bond-clad compatibility.

II. EBR-II IRRADIATION TESTING
(J. O. Barner)

A. General

The purpose of the EBR-II irradiations is to evaluate candidate fuel/sodium/clad fuel element systems for the LMFBR program. In the reference design, fuel pellets of single-phase (U,Pu)C are separated by a sodium bond from a cladding of Type 316 stainless steel. Three series of experiments are planned and approval-in-principle has been received from the AEC.

The capsules are to be irradiated under the following conditions:

Condition	Series 1	Series 2	Series 3
1. Lineal power, kW/ft	~ 30	~ 45	~ 30
2. Fuel composition	$(U_{0.8}Pu_{0.2})C$, single-phase, sintered		
3. Fuel uranium	^{235}U	^{233}U	^{235}U
4. Fuel density	90%	95%	95%
5. Smear density	80%	80%	80%
6. Clad size	0.300-in. i.d. x 0.010-in. wall		
7. Clad type	316 SS	316 SS	316 SS
8. Max clad temp, °F	1250	1275	1250
9. Max fuel centerline temp, °F	2130	2550	2100
10. Burnup	3 a/o to 8 a/o		

The capsules are doubly contained.

B. Current Results

Two capsules from Series 1, designated K-42B and K-36B are assembled in EBR-II subassembly X070. They will be inserted in the reactor for Run 39B in mid-January 1970.

Three capsules from Series 1, designated K-37B, K-38B, and K-39B, and two capsules from Series 3, designated K-43 and K-44, are available for irradiation. They will be inserted when EBR-II project personnel have reviewed the "data package."

The data package for the Series 1 and 3 irradiations is almost complete. The results of temperature calculations for capsules with assumed sodium bond discontinuities must be obtained to complete the data package.

III. THERMAL IRRADIATIONS OF SODIUM-BONDED MIXED CARBIDES

(J. C. Clifford, R. L. Cubitt, D. C. Kirkpatrick)

A. General

Mixed carbides, sodium-bonded to Type 316 stainless steel cladding, are being irradiated in the LASL Omega West Reactor (OWR), a 6 MW MTR-type facility. The purpose of the experiments is to determine whether fuel, clad, and sodium remain mutually compatibile as burnups of interest in the LMFBR program are approached. While fast-spectrum irradiations are preferred in order to produce the power densities and radial temperature gradients anticipated in LMFBRs, thermal irradiations appear acceptable in this instance because the fuel regions of prime interest (those in contact with sodium) for compatibility studies can be maintained at realistic temperatures.

Experiments are conducted in instrumented environmental cells installed semi-permanently in the OWR. The principal features of these cells are: (1) a heat removal and temperature control system consisting of a natural convection sodium loop, electrical heaters, and a variable conductivity heat leak, and (2) a sweep gas system for the rapid detection of leaking fuel capsules.

B. Current Results

A second environmental cell, fabricated during the previous quarter, was installed in the OWR. A dummy experiment, containing stainless steel in lieu of fuel, was operated in the cell for two weeks to ensure that control and alarm circuitry were functioning and to measure the heat generated by gamma photon absorption in cell components.

OWREX-14, a sodium-bonded $(U_{0.8}Pu_{0.2})C$ experiment, was inserted in the new cell early in December and has operated satisfactorily since that time. The experiment consists of two Type 316 stainless steel capsules, each 2.5-in. long and 0.300-in. diam with 0.010-in.-thick walls. Each capsule contains three pellets of 95% theoretical density, single-phase mixed carbide, a stainless steel insulator pellet to separate the fuel from the lower closure weld, and approximately 1/3 g Na. The uranium in the fuel is fully enriched in ^{235}U.

The capsules are stacked end on end at the axial center of a 0.600-in.-diam stainless steel secondary container. The annular volume between capsules and secondary is filled with sodium, and capsules are centered in the secondary by thin stainless steel disks at the top and base of each capsule. The experiment contains eight thermocouples for monitoring temperatures of the fuel capsules and secondary sodium.

Based on measurements of the electrical power required to maintain the experiment at a fixed temperature with and without nuclear heat, the fuel capsules are estimated to generate 3 kW of fission heat at reactor operating power. Using computed integral power and radial power distribution, and normalizing the former to the measured power generation, the resulting specific power at the fuel surface is 670 W/g of fuel and the average is 168 W/g. Fuel pellet surfaces are operating in the range 600-700°C. At the end of December, the experiment had reached ~ 20% of a planned skin burnup of 4 a/o.

Assembly of OWREX-15, a duplicate of the carbide experiment just described, has been completed and the experiment will be inserted in the OWR in mid-January. This experiment will occupy the cell vacated recently after the termination of a U-Pu-Zr experiment (Section IV). OWREX-15 is planned for operation to 8 a/o skin burnup, requiring ~ 110 days of reactor operation.

IV. THERMAL IRRADIATIONS OF SODIUM-BONDED U-Pu-Zr

(J. C. Clifford, R. L. Cubitt, D. C. Kirkpatrick)

A. General

Thermal irradiations are conducted to evaluate the behavior of U-Pu-Zr alloys produced by LASL. Irradiations are conducted at the Omega West Reactor in an environmental cell in which temperature changes accompanying reactor power level changes are minimized with electrical heat and with a variable conductivity heat leak. Using this cell, it is possible to minimize thermal cycling of the fuel through phase transformations that affect its swelling behavior.

Complementary to the irradiations is an out-of-pile investigation of the compatibility of LASL-produced U-Pu-Zr alloys with Type 316 stainless steel and with a vanadium alloy. Of prime interest is the effect of zirconium and oxygen content of the fuel on reactions between fuel and stainless steel in the temperature range 600-750°C.

B. Current Results

1. Irradiation Experiments

The most recent metal fuel experiment, OWREX-13, failed prematurely and has been removed from the reactor. The experiment has been radiographed and shows evidence of significant fuel relocation in all three fuel capsules. Destructive examination of this experiment and of the previous U-Pu-Zr failure will be accomplished as the hot cell schedule permits. In view of the rapidity of the failures, the decline of interest in metals as LMFBR fuels, and the recent decrease in OWR power level, additional metal fuel experiments are unlikely. The environmental cell used for the metal fuel irradiations will be used for irradiation of mixed carbides (Section III) beginning in mid-January.

2. Compatibility Experiments

Procedures have been established, equipment is available, and materials are on hand for a limited number of compatibility tests employing LASL-produced U-Pu-Zr alloys and stainless steel. Assembly of fuel and stainless steel specimens into presses has been started. Testing will be completed by the end of the fiscal year.

PROJECT 501

STANDARDS, QUALITY CONTROL, AND INSPECTION OF PRODUCTS

Person in Charge: R. D. Baker
Principal Investigator: C. F. Metz

I. INTRODUCTION

A major factor in the development of a successful reactor fuel is a high degree of technical competence for doing the required chemical analysis and related measurements necessary to characterize thoroughly the raw materials, the manufactured fuel, and the irradiated fuel. This project is identified with the mixed oxide fuel development phase of the LMFBR/FFTF Program.

This project is directed toward (1) developing an analytical chemistry and measurements program, thereby ensuring high quality and uniformity of raw materials, (2) establishing and conducting a statistically designed quality control program of chemical analyses and other measurements that can be used to assure continuing adequate analytical competence of the fuel producers during the fuel fabrication stage, and (3) doing correlated chemical analyses and related measurements on irradiated fuel as a means of studying fuel behavior during core life; specifically involved will be burnup studies correlated with microprobe and metallography studies, gas release studies as related to cladding corrosion, and gas retention studies as related to porosity, particle size, and other properties of the fuel.

II. FFTF ANALYTICAL CHEMISTRY PROGRAM

The remainder of the data for Phase II of the analytical program, as outlined in LASL Document CMB-1-870, was received from some participants who had not finished their work previously due to operational problems. Statistical analyses are being completed, and a final report describing Phase II results is in preparation.

III. INVESTIGATION OF METHODS

An important part of the analytical chemistry program is the investigation and improvement of analytical methods, or development of new methods. The following were investigated:

1. Determination of F in Sintered $(U,Pu)O_2$
(T. K. Marshall)

Trace concentrations of F, which may significantly affect corrosion rates of stainless steel cladding materials, are measured reliably with a fluoride ion specific electrode following pyrohydrolytic separation from the sintered oxides. Results obtained for 1 to 10 μg of F added to 1-g portions of U_3O_8, used as a stand-in for $(U,Pu)O_2$, show that recovery of fluoride is 97 percent and the relative precision (1 σ) is 4 percent for a single determination.

Testing of the method was completed by making repeated measurements of 1 to 9 μg of F added as a solution of KF to 1-g portions of $(U,Pu)O_2$. The $(U,Pu)O_2$ used in preparing these samples was freed of traces of fluoride by a pyrohydrolysis treatment before addition of the KF. Results for the repeated analyses showed an average recovery of 104 percent of the F^- and relative standard deviations (1 σ) of 5 percent for a single measurement of 2 to 9 μg of F^- and 6 percent for 1 μg of F^-. The reliability of the method was considered adequate for the small quantities determined.

2. O/M Ratios in Sintered $(U,Pu)O_2$
(G. C. Swanson, T. K. Marshall, G. R. Waterbury)

The O/M atom ratio is an important chemical property that is included in the tentative FFTF fuel

specifications. Quantitative measurement of this property by thermogravimetric methods is under investigation. In one proposed method,[1] the sample is oxidized in air at 750°C and then reduced in He-6% H_2 at 700°C to the stoichiometric dioxide. The O/M ratio is calculated from the initial and final weights. Previous work showed that a reduction temperature of 1000°C was required to obtain an oxide product that was essentially stoichiometric (O/M of 2.001). The effects of various reduction temperatures on the compositions of the final oxides were determined by repeatedly analyzing 3:1 mixtures of UO_2 and PuO_2, prepared from very high purity metals (> 99.99% pure). The O/M ratios of the oxides produced were:

Reduction Temperature, °C	O/M Ratio of Product
700	2.016
800	2.011
900	2.005
1000	2.001

Extrapolation of a plot of these data indicated that stoichiometry should be attained at 1015°C.

The effects of other procedural changes also were determined. In each case oxides prepared from pure metals were used as samples. In the original proposed method, oxidation of the sample was accomplished by removing the furnace end cap to allow air to back diffuse onto the sample heated to 750°C. It was found that samples were oxidized adequately and easily by leaving the furnace end cap off as the furnace was being heated from room temperature up to the 1000°C reduction temperature.

The length of the reduction period at 1000°C was found to be critical. Hyperstoichiometric oxides reduced in He-6% H_2 at 1000°C for 2, 4, 5, and 6 hours had O/M ratios of 2.006, 2.002, 2.002, and 2.000 respectively. Previous work showed that additional time, up to 18 h, at 1000°C did not cause further reduction of the oxide. A reduction period of 6 h was selected as optimum.

Decreasing the flow of reducing gas from 2 ℓ/min to 1 ℓ/min did not affect the results. The final O/M ratios of 12 prepared mixed oxides averaged 2.001 with a standard deviation (1σ) of 0.002 when the flow rate was 1 ℓ/min curing the 6 h reduction at 1000°C.

The effects on the method of several added impurities, including, C, Fe, Al_2O_3, Al, CaO, and Na_2SO_4, are being investigated.

Plots of sample weight versus temperature obtained for small UO_2 samples by an automatic microthermogravimetric analysis apparatus showed also that O/M ratios near 2.000 were obtained at 1000°C in dry He-6% H_2. Some scatter in the data was attributed to differences in the compositions of the initial small UO_2 samples. Cycling of one UO_2 sample through oxidations and reductions to produce several thermograms was started to determine the cause of the poor reproducibility.

In another proposed thermogravimetric method,[2] the sample is reacted at 800°C with Ar-8% H_2 containing 4 mm partial pressure of H_2O to form the stoichiometric dioxide. These conditions produced hyperstoichiometric oxides from unsintered UO_2, PuO_2, or a UO_2-PuO_2 mixture, prepared from the pure metals; the O/M ratios were between 2.016 and 2.019. At a reaction temperature of 1000°C, the O/M ratio of the 3:1 UO_2PuO_2 mixture was reduced to 2.008, and cooling the sample in dry Ar from reaction temperature (1000°C) to room temperature for weighing reduced the average O/M ratio to 2.006. At the present time an induction heater is being used to study the effects on the O/M ratio of reduction temperatures between 1000°C and 1250°C.

3. Gas evolution from Sintered $(U,Pu)O_2$
(D. E. Vance and M. E. Smith)

The internal pressures developed in sealed reactor fuel capsules are dependent to a significant extent on the quantities of gases, including H_2O vapor, evolved from the fuel at operating temperatures. To determine the amount of gases obtained from sintered mixed-oxide pellets, the H_2O released at 800°C was measured separately from the other gases evolved at 1600°C. In the method for measuring H_2O, the sintered mixed-oxide pellet was heated in a fused-silica furnace tube at 800°C, and the evolved H_2O was swept by Ar to a moisture monitor. Integration of the monitor signal gave a quantitative measure of the H_2O. Reliable determinations of H_2O were made on several pellets and the apparatus functioned

reliably. Investigation was continued with the goal of making minor improvements in the operations and equipment.

It was found during periodic calibrations of the apparatus that the useful life of the sensor cell in the moisture monitor was extended by maintaining a small positive gas pressure in the cell. As the positive pressure did not adversely affect the measurements, this change in operation has been followed.

A new calibration method is being tried to avoid the adsorption difficulties associated with injections of water. A stainless steel tube filled with CuO and heated to 550°C was installed between the fused-silica furnace and the moisture monitor. Measured quantities of H_2 injected into the apparatus are oxidized to water by the CuO and measured by the moisture monitor. The method is promising, and a series of H_2 injections are in progress to test this calibration of the apparatus.

Determination of gases other than H_2O is accomplished by a vacuum extraction technique in which a fuel pellet is heated inductively in a W crucible to 1600°C. The gases evolved are pumped from the furnace through a $Mg(ClO_4)_2$ desiccant and collected by a Toeppler pump. The total volume of gas under standard conditions is calculated from the measured volume, temperature, and pressure of the gas. Initial tests of the method were satisfactory, but changes in the construction of the first analysis apparatus seemed advisable to ensure trouble-free operation. A new type of induction furnace was designed and fabricated to eliminate diffusion leaks and provide higher temperatures. An all-stainless-steel vacuum manifold, which was nearly impervious to Hg vapor, was being constructed. When these components are completed and tested, work will be resumed on the determination of evolved gases.

4. Spectrochemical Analysis of UO_2 and PuO_2
(W. M. Myers, C. J. Martell, C. B. Collier, and R. T. Phelps)

Control of the impurity elements in sintered $(U,Pu)O_2$ depends on the purity of the starting UO_2 and PuO_2, and requires reliable spectrochemical analyses of these raw materials. Impurity analysis of PuO_2 was started by preparing PuO_2 standards containing the elements whose maximum concentration levels have been specified in the fuel. Two sets of the standards were required because two methods of analysis were needed in order to have adequate detection sensitivity fo all specified impurities.

In one method, 22 impurity elements (Ag, Al, B, Ba, Be, Bi, Ca, Cd, Cr, Cu, Fe, Li, Mg, Mn, Na, Ni, P, Pb, Si, Sn, Sr and Zn) are determined by a carrier-distillation technique. The electrode charge contains 4% Ga_2O_3 to serve as the carrier and 500 ppm of Co as an internal standard. Although this method is used for routine analysis of Pu for 12 elements, further investigation is required to evaluate its use for determi ning 22 elements.

In the second method, Nb, Mo, Ti, V, W plus Co are determined, also by a carrier-distillation technique but with 50% AgCl added to the electrode charge to serve as the carrier. The AgCl contains some $PdCl_2$ to serve as an internal standard. The 50-mg electrode charge is arced in an O_2 atmosphere, and the characteristic spectra obtained using a high-dispersion spectrograph are photographed. The relative precision (1 σ) is 20% in determining the six elements in the nominal concentration range of 10 to 500 ppm. The detection limits are Co-2 ppm, Mo-3, Nb-10, Ti-5, V-1 and W-5. These data show that the method is satisfactory for the determination of these elements in PuO_2.

Further evaluation of the method for analysis of 22 elements in PuO_2 and studies of methods to analyze UO_2 are planned.

5. Measurement of N_2 in $(U,Pu)O_2$
(G. C. Swanson)

One of the impurity elements in FFTF fuels for which a specification exists is N_2. Analysis for this impurity generally involves a tedious dissolution of the sample under conditions that allow neither loss nor pick-up of N. One advantage of a LECO Nitrox-6 Analyzer is that solid samples are analyzed. The sample is heated inductively in a C crucible to 1900 to 2100°C to liberate N_2 which is measured in a simple gas chromatograph system. Under these conditions, the O in the oxide sample forms

large quantities of Co which interfere in the measurement of N_2. A heated tube containing CuO to oxidize the CO and an Ascarite trap for CO_2 were installed immediately before the gas chromatographic column. This system removes essentially all of the CO and permits sensitive determinations of N_2.

Calibration of the apparatus using prepared samples of UO_2 containing known amounts of added U_2N_3 was started. Some difficulties in obtaining reproducible recoveries of N from these standards were traced to the heating cycle. A slower initial heating rate proved beneficial, and calibration was resumed.

IV. REFERENCES

1. W. L. Lyon, GEAP-4271, 1963.
2. T. D. Chikalla, in "Quarterly Progress Report, October-December 1966," F. W. Albaugh et al, pp 4.1, BNW-L-cc-957, 1967.

SPECIAL DISTRIBUTION

Atomic Energy Commission, Washington

Division of Research

D. K. Stevens

Division of Naval Reactors

R. H. Steele

Division of Reactor Development and Technology

G. W. Cunningham
D. E. Erb
Nicholas Grossman
W. H. Hannum (2)
K. E. Horton
J. R. Humphreys
R. E. Pahler
J. M. Simmons (2)
E. E. Sinclair
Bernard Singer
C. E. Weber
G. W. Wensch
M. J. Whitman

Division of Space Nuclear Systems

G. K. Dicker
F. C. Schwenk

Safeguards & Materials Management

J. M. Williams

Idaho Operations Office

DeWitt Moss

Ames Laboratory, ISU

O. N. Carlson
W. L. Larsen
M. Smutz

Argonne National Laboratory

F. G. Foote
Sherman Greenberg
J. H. Kittel
W. B. Loewenstein
R. E. Macherey
M. V. Nevitt
R. C. Vogel

Idaho Falls, Idaho

D. W. Cissel
R. C. Robertson

Atomics International

R. W. Dickinson, Director (2)
Liquid Metals Information Center

J. L. Ballif

Babcock & Wilcox Co.

C. Baroch
J. H. MacMillan

Battelle Memorial Institute

D. L. Keller
S. J. Paprocki

Brookhaven National Laboratory

D. H. Curinsky
C. Klamut

Combustion Engineering, Inc.

S. Christopher

Donald W. Douglas Laboratories

R. W. Andelin

General Electric Co., Cincinnati, Ohio

V. P. Calkins

General Electric Co., Sunnyvale, California

R. E. Skavdahl

Gulf General Atomic, Inc.

E. C. Creutz

Idaho Nuclear Corporation

W. C. Francis

IIT Research Institute

R. Van Tyne

Lawrence Radiation Laboratory

Leo Brewer
J. S. Kane
A. J. Rothman

LMFBR Program Office

D. K. Butler (Physics)
P. F. Gast
L. R. Kelman (Fuel & Materials)
J. M. McKee (Sodium Technology)

Mound Laboratory

R. G. Grove

NASA, Lewis Research Center

J. J. Lombardo

Naval Research Laboratory

L. E. Steele

Oak Ridge National Laboratory

G. M. Adamson
J. E. Cunningham
J. H. Frye, Jr.
C. J. McHargue
P. Patriarca
O. Sisman
M. S. Wechsler
J. R. Weir

Pacific Northwest Laboratory

F. W. Albaugh
E. A. Evans
V. J. Rutkauskas
W. R. Wykoff

FFTF Project

E. R. Astley
B. M. Johnson
D. W. Shannon (2)

U. S. Department of Interior

Bureau of Mines, Albany, Oregon

H. Kato

United Nuclear Corporation

A. Strasser

Westinghouse, Advanced Research Division

E. C. Bishop

Australian Atomic Energy Commission

J. L. Symonds